

# Synthesis of Fatty Acid Binding Protein Inhibitors: A New Approach for Diabetes Treatment

Shekelia Baccus, M. Perry Davis, Jr., and David R. Magnin<sup>a</sup>

Morris College, Division of Natural Sciences and Mathematics, 100 West College Street. Sumter, SC 29150

Received September 17, 2009

Adipocyte fatty acid binding protein (aFABP, aP2) is a 14.6 kDa cytosolic protein located in adipocytes and macrophages and assists in the intracellular transport of fatty acids. It is one of a class of fatty acid binding proteins (FABPs) that are found predominately in the liver, heart, intestine and connective tissues. Hotamisligal *et al.* have reported that aFABP-deficient mice, when placed on a high fat diet (40% of caloric intake as fat), were significantly protected from hyperinsulinemia and insulin resistance compared to the wild type. Additional genetic experiments have been reported in which aFABP null mice have been crossed with *ob/ob* and in another instance apoE<sup>-/-</sup> mice. The aFABP-deficient *ob/ob* mice were more insulin sensitive when compared to *ob/ob* controls as demonstrated measuring by circulating glucose and insulin levels. Based on these genetic knock-out models, we pursued the development of inhibitors of aFABP for their therapeutic potential in the treatment of diabetes. Herein we disclose the synthesis of twoazole inhibitors of P2 and the methods used to prepare them

## Introduction

With the spread of Western lifestyles, the prevalence of type 2 diabetes is rising. In the United State it is estimated that nearly 21 million children and adults (7.0% of the population) have diabetes. Of this number only 15 million are currently diagnosed. Alarmingly, it is also estimated that there are potentially 54 million people who are currently “pre-diabetic”. This is a situation where glucose is only partially controlled. If the situation is left unmanaged it is anticipated that these individuals will ultimately exhibit the disease. Taken together, there are 1.5 million new cases of diabetes being diagnosed in people aged 20 years or older (2005 data) within the United States each year. The expectation is that these numbers are likely to greatly increase in the near future.<sup>1</sup>

Diabetes is characterized by hyperglycemia and disturbances of carbohydrates, lipid and protein metabolism. As these metabolic disturbances become “chronic,” a wide variety of medical problems present themselves. Foremost among them these are heart disease and stroke accounting for 65% of deaths in people with diabetes. In addition, a high percentage of diabetics are afflicted with hypertension. Diabetic complications are not limited to cardiovascular concerns. Diabetes also has a detrimental impact on the retina, kidney and nervous systems. The disease becomes the basis for 24,000 new cases of blindness annually, nearly half of new cases of kidney failure, and a major percentage of lower limb amputations;<sup>2</sup> the total cost of the disease is currently estimated at over 150 billion dollars in the United States annually.<sup>1</sup>

Current diabetes treatment strategies include: reducing insulin resistance using glitazones,<sup>3</sup> supplementing insulin supplies with exogenous insulin,<sup>4</sup> increasing insulin secretion with sulfonyl ureas,<sup>5</sup> and reducing hepatic glucose production with biguanides.<sup>6</sup> Recently, treatment strategies using DPP-IV inhibitors and GLP-1 agonists<sup>7</sup> have also emerged. Of the aforementioned list, the mechanisms of action generally focus on treating type 2 diabetes predominately from the glucose/insulin axis. However, there is currently no chemical agent that addresses diabetes via altered energy homeostasis from the fatty

acid vantage point. By altering the modulation of energy stores along the fatty acid axis an impact on circulating glucose levels would be expected. This strategy then provides a new basis for therapy.

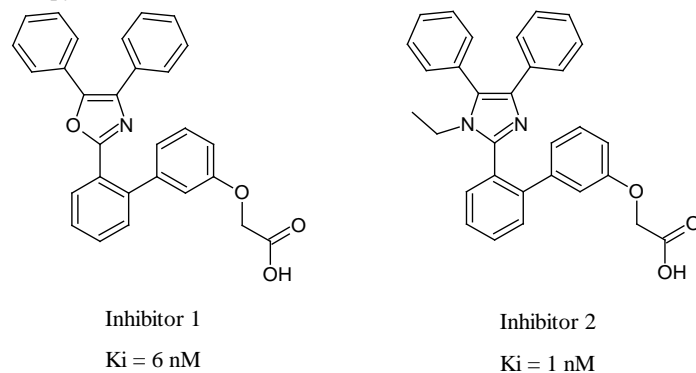


Figure 1: Potent Inhibitors of aP2

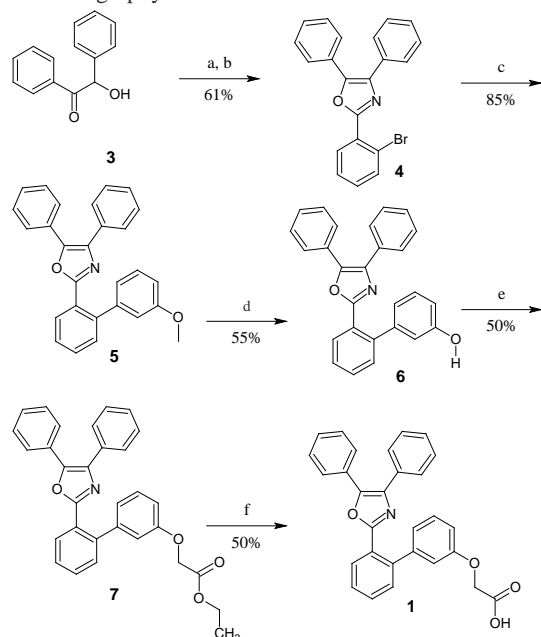
A promising new diabetes target for investigation is the inhibition of aP2.<sup>8</sup> aP2 is one of a family of homologous intracellular fatty acid binding proteins that is involved in the regulation of fatty acid trafficking. aP2 is found in adipocytes and mediates fatty acid fluxes in adipose tissue.<sup>9</sup> Hotamisligal *et al.* have reported that aFABP deficient mice, when placed on a high fat diet (40% of caloric intake as fat), were significantly protected from hyperinsulinemia and insulin resistance compared to the wild type.<sup>10</sup> Additional genetic experiments have been reported in which aFABP null mice have been crossed with *ob/ob* mice. The aFABP deficient *ob/ob* mice were more insulin sensitive when compared to *ob/ob* controls as demonstrated measuring by circulating glucose and insulin levels.<sup>11</sup> Supported by these genetic knock-out models, aP2 inhibition presents itself as an perfect target for the treatment of diabetes.<sup>9</sup> Moreover, workers at Harvard and Bristol-Myers Squibb recently reported successful intervention with an aP2 inhibitor against a wide variety of diabetes markers including fasting and parandial glucose levels in the *ob/ob* mouse.<sup>12</sup>

There are several reports of aP2 inhibitors in the literature;<sup>11</sup> these papers typically reveal binding affinities to aP2 and very limited chemical synthetic procedures. Our goal was to

prepare two known potent inhibitors of aP2<sup>12</sup> (**Figure 1**) and disclose needed experimental details to provide access in determining if these agents would serve as forerunners of a new therapeutic class of anti-diabetic agents. For this reason the preparation of the two compounds below was undertaken. They both have high binding affinity to aP2. The first compound was prepared according to the methods in **Scheme 1**. The second compound was prepared as seen in **Scheme 2**.

### Chemistry:

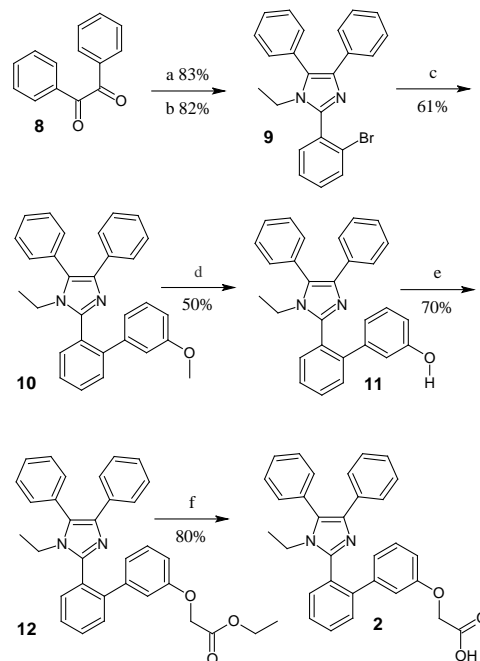
In **Scheme 1**, benzoin (**3**) was reacted with 2-bromo-benzoic acid under standard conditions to give benzoin 2-bromobenzoate. The ester was reacted without purification and immediately treated with ammonium acetate in acetic acid to generate oxazole **4** (45% overall). Compound **4** smoothly underwent palladium catalyzed cross coupling with 3-methoxyphenyl boronic acid in 75% isolated yield. Deprotection of the methyl group was achieved with BBr<sub>3</sub> to provide hydroxyl-biphenyl **6**. For this conversion, maintaining the reaction temperature below 0 °C proved to be critical in the successful transformation of the ether to the alcohol. Warmer temperatures and prolonged reaction times generated multiple side products. Isolated yields of the alcohol were around 55%. The final two steps in generating the target inhibitor required coupling of the phenol with ethyl bromoacetate (DMF and K<sub>2</sub>CO<sub>3</sub>, 65%), followed by hydrolysis of the ester (KOH in alcohol 50%) to provide the target molecule (**1**). Isolation of the salt was accomplished with the agency of SP207 gel column chromatography.



**Scheme 1:** a. (COCl)<sub>2</sub>, 2-bromobenzoic acid; b. NH<sub>4</sub>OAc, HOAc, Δ; c. methoxyphenyl boronic acid, Pd(PPh<sub>3</sub>)<sub>4</sub>, Na<sub>2</sub>CO<sub>3</sub>; d. BBr<sub>3</sub>, -5 °C; e. ethyl bromoacetate, K<sub>2</sub>CO<sub>3</sub>; f. NaOH.

Compound **2** was prepared as outlined in **Scheme 2**. 2-Bromo-benzaldehyde was reacted with diketone **8** to form an imidazole. The imidazole ring was then alkylated with ethyl iodide in the presence of K<sub>2</sub>CO<sub>3</sub> to give **9** (65% overall). Compound **9** was reacted with palladium (0) tetrakis(triphenyl-

phosphine under Suzuki conditions generating biphenyl **10**. The yields of the reaction tended to vary but averaged around 70%. The methyl ether in **10** was deprotected with boron tribromide with reaction temperatures below 0 °C to liberate phenol **11** (yields 35%-50%). The target molecule **2** was prepared by K<sub>2</sub>CO<sub>3</sub>/DMF and ethyl bromoacetate coupling followed by base hydrolysis. Overall conversions were around 35% for the last two procedures.



**Scheme 2:** a. NH<sub>4</sub>OAc, HOAc, 2-bromo-benzaldehyde; b. ethyl iodide, K<sub>2</sub>CO<sub>3</sub>; c. methoxyphenyl boronic acid, Pd(PPh<sub>3</sub>)<sub>4</sub>, Na<sub>2</sub>CO<sub>3</sub>; d. BBr<sub>3</sub>, -5 °C; e. ethyl bromoacetate, K<sub>2</sub>CO<sub>3</sub>; f. NaOH

### Materials and Methods

Reagents were purchased from Aldrich Chemical (P.O. Box 2060 Milwaukee, WI 53201) and used without further purification. All column chromatography was carried out using ACROS silica gel 0.20 -0.50 mm, pore diameter – 4 nm. TLC was carried out on Merk Silica Gel Plates with a UV binder. Typical visualization was accomplished by UV, I<sub>2</sub> or KMnO<sub>4</sub> staining. <sup>1</sup>H NMR was carried out on an Anasazi EFT-60 MHz Spectrometer referenced to TMS. HPLC was carried out using Waters 1525 HPLC. Column: Waters X-Terra Phenyl: pore 5μm, length 4.6X150mm. UV detection at 220 and 245 nm. A linear gradient from 100% solvent A to 100% solvent B was run from time 0 min. to time 16 min. Solvent A: (water:methanol:acetic acid; 9/1/.025), Solvent B (water:methanol:acetic acid; 1/9/.025). SP207 gel was purchased from Sorbent Technologies (2377 John Glen Dr. Atlanta, GA 30341) and used after washing with solutions of NaOH, HCl, water, methanol, and acetone. The resin was stored over a solution of very dilute NaHCO<sub>3</sub>:methanol solution (95:5 v/v).

### Preparation of 2-(2-bromophenyl)-4,5-diphenyl-1,3-oxazole (**3**).

A solution of 2-bromobenzoic acid (5.00 g, 24.77 mmol) and dichloromethane (50 mL) was treated with oxaly

chloride (3.81g, 30.00 mmol) and dimethyl formamide (5 drops). The reaction mixture was stirred until all gas evolution has stopped (0.5 h). The mixture was stripped on a rotoevaporator and the remaining acid chloride diluted with dichloromethane (100 mL). The slight yellow solution was mixed with benzoin (4.64 g, 22.00 mmol) and triethylamine (7.50, 75.00 mmol). The mixture was stirred overnight and diluted with water. The layers were separated and the dichloromethane fraction washed with Na<sub>2</sub>CO<sub>3</sub> solution and then KHSO<sub>4</sub>. The organics were dried over MgSO<sub>4</sub> and concentrated to give the ketoester as a colorless oil.

The crude ester (3.60 g, @ 9.4 mmol) from above was mixed with ammonium acetate (3.60 g, 47 mmol) and acetic acid (35 mL). The mixture was brought to reflux for 4 h and cooled to ambient temperature. The organics were diluted with ethyl acetate and water. The layers equilibrated and separated. The organic fraction was washed with water, NaHCO<sub>3</sub>, brine, dried (MgSO<sub>4</sub>) and concentrated to give yellow oil. The oil was recrystallized from a small volume of hot methanol to give the desired oxazole (2.20 g, 61%). TLC (1:3 ethyl acetate/hexane) R<sub>f</sub> = 0.4; <sup>1</sup>H NMR (CDCl<sub>3</sub>) δ 8.20 -6.90 (m, 14 H) ppm.

#### **Preparation of 2-(2-(3-methoxyphenyl)-phenyl)-4,5-diphenyl-1,3-oxazole (4).**

Nitrogen was bubbled through a solution of **3** (0.29 g, 0.78 mmol), 3-methoxy-phenyl boronic acid (0.15 g, 0.98 mmol) and aqueous Na<sub>2</sub>CO<sub>3</sub> (0.7 mL, 2M) in toluene (3 mL) and ethanol (0.85mL) for about 10 min. Tetrakis (triphenylphosphine) palladium (0) (50 mg) was added and the reaction was heated in an oil bath set at 77 for 14 h. The mixture was cooled and diluted with ethyl acetate (25 mL) and the organics were washed with water, NaHCO<sub>3</sub>, dried and concentrated. The remainder was purified on silica gel column chromatography with 1:5 ethyl acetate in hexanes as a mobile phase. The procedure provided 0.27 g (85%) of the title compound. TLC (1:3 ethyl acetate/hexane) R<sub>f</sub> = 0.7; <sup>1</sup>H NMR (CDCl<sub>3</sub>) δ 8.20 -6.90 (m, 18 H), 3.50 (s, 3H) ppm.

#### **2'-(4,5-diphenyl-1,3-oxazol-2-yl)biphenyl-3-ol (5).**

To a solution of **4** (0.25 g, 0.62 mmol) in anhydrous dichloromethane at -10°C was added boron tribromide in dichloromethane dropwise (2M, 0.65 mL). The reaction was stirred at -5°C for 1 h and quenched with aqueous NaHCO<sub>3</sub> solution and the pH adjusted to 6 with dilute HCl. The mixture was diluted with ethyl acetate and the organics separated from the aqueous fraction. The organics were washed with brine, dried over MgSO<sub>4</sub> and concentrated. The remainder was purified on silica gel column chromatography with dichloromethane and then 10% ethyl acetate/dichloromethane to give the title compound (0.10 g, 55%). TLC (1:3 ethyl acetate/hexane) R<sub>f</sub> = 0.3; <sup>1</sup>H NMR (CDCl<sub>3</sub>) δ 8.20 -7.00 (m, 18 H), 1.90 (s broad, 1H) ppm.

#### **Ethyl [[2'-(4,5-diphenyl-1,3-oxazol-2-yl)biphenyl-3-yl]oxy]acetate (6).**

A 25 mL RB flask was charged with DMF (2.5 mL), K<sub>2</sub>CO<sub>3</sub> (0.055 g, 0.04 mmol), ethyl bromoacetate (0.038 g, 0.02 mmol) and compound **5** (0.080 g; 0.20 mmol). The biphasic

mixture was stirred overnight and diluted sequentially with ethyl acetate 15 mL and water 15 mL. The layers were separated and the organic fraction was washed with water, dried over Na<sub>2</sub>SO<sub>4</sub> and concentrated. The remainder was purified by silica gel column chromatography with ethyl acetate and hexanes as a mobile phase. A gradient elution from hexane to 25% ethyl acetate in hexane provided the title compound. (0.80 g, 50%-85%). TLC (1:3 ethyl acetate/hexane) R<sub>f</sub> = 0.5; <sup>1</sup>H NMR (CDCl<sub>3</sub>) δ 7.90 -6.80 (m, 18 H), 4.60 (s, 2H), 4.20 (q, 2H, J=7.5 Hz), 1.60 (t, 3H, J=7.5 Hz) ppm.

#### **[[2'-(4,5-diphenyl-1,3-oxazol-2-yl)biphenyl-3-yl]oxy]acetic acid, sodium form (1) Inhibitor 1.**

A 25 mL RB flask was charged with ethanol (7 mL), NaOH (0.4 g, 10 mmol), compound **6** (0.80 g, 0.16 mmol) and 1 mL of water. The mixture was heated to reflux for 6 h and cooled to room temperature. The mixture was concentrated and purified on SP207 gel using a step gradient with 100 mL volumes starting with water; 10% methanol in water; 20% methanol in water; 30% methanol in water; 50% methanol in water; 75 % methanol in water; 90% methanol in water; and methanol to give 0.18 g of final product. TLC (1:3 ethyl acetate/hexane) R<sub>f</sub> = 0.05; HPLC: Retention Time: 15.4 min. <sup>1</sup>H NMR (CD<sub>3</sub>OD) δ 7.90 -6.80 (m, 18 H), 4.50 (s, 2H) ppm.

#### **2-(2-bromophenyl)-4,5-diphenyl-1H-imidazole (8a).**

Benzil (**8**) (4.20 g, @ 20.0 mmol) was mixed with ammonium acetate (14.40 g, 188 mmol), acetic acid (45 mL) and 2-bromo-benzaldehyde (3.70 g, 20.0 mmol). The mixture was brought to reflux for 14 h and cooled to ambient temperature. The organics were diluted with a large volume of water and a white solid formed. The solid was collected by filtration and dried overnight. After standing overnight the material maintained a strong acetic acid odor. The solid was then triturated with water and filtered three times to remove any acetic acid and/or ammonium salts. The solid collected provided the title compound (6.20 g, 83%). TLC (1:3 ethyl acetate/hexane) R<sub>f</sub> = 0.5; <sup>1</sup>H NMR (CDCl<sub>3</sub>) δ 8.20-7.20 (m, 14 H), 1.80 (s broad, 1H) ppm.

#### **2-(2-bromophenyl)-1-ethyl-4,5-diphenyl-1H-imidazole (9).**

To a mixture of **8a** (2.5 g; 6.70 mmol), K<sub>2</sub>CO<sub>3</sub> (1.33 g; 10.00 mmol) and DMF (20 mL) was added ethyl iodide (1.40 g; 8.80 mmol). The mixture was stirred overnight and diluted with water. After vigorous stirring a white solid was formed. The solid was collected by filtration and dried overnight. The material was triturated with water two times and the resulting solid collected by filtration. The solid collected provided the title compound (2.19 g, 82%). TLC (1:3 ethyl acetate/hexane) R<sub>f</sub> = 0.6; <sup>1</sup>H NMR (CDCl<sub>3</sub>) δ 7.80 -7.00 (m, 14 H), 3.75 (q, 2H, J=11.5 Hz), 0.95 (t, 3H, J=11.5 Hz) ppm.

#### **1-ethyl-2-(3'-methoxybiphenyl-2-yl)-4,5-diphenyl-1H-imidazole (10).**

Nitrogen was bubbled through a solution of **9** (0.35 g, 0.81 mmol), 3-methoxy-phenyl boronic acid (0.15 g, 0.98 mmol) and aqueous Na<sub>2</sub>CO<sub>3</sub> (0.7 mL, 2M) in toluene (3 mL) and ethanol (0.85 mL) for about 10 min. Tetrakis (triphenylphosphine) palladium (0) (50 mg) was added and the

reaction was heated in an oil bath set at 70°C for 14 h. The mixture was cooled and diluted with ethyl acetate (25 mL) and the organics were washed with water, NaHCO<sub>3</sub>, dried and concentrated. The remainder was purified on silica gel column chromatography with 1:5 ethyl acetate in hexanes as a mobile phase. The procedure provided (0.23 g, 61%) of the title compound. TLC (1:3 ethyl acetate/hexane) R<sub>f</sub> = 0.8; <sup>1</sup>H NMR (CDCl<sub>3</sub>) δ 7.80-6.90 (m, 18 H), 3.60 (s, 2H), 3.20 (q, 2H, J=8.5 Hz), 0.60 (t, 3H, J=8.5 Hz) ppm.

#### **1-ethyl-2-(3'-hydroxybiphenyl-2-yl)-4,5-diphenyl-1H-imidazole (11).**

To a solution of **10** (0.25 g, 0.62 mmol) in anhydrous dichloromethane at -10 °C was added boron tribromide in dichloromethane drop wise (2M, 0.65 mL). The reaction was stirred at -10°C for 90 min. and quenched with methanol (2 mL). The mixture was stirred for 1 h at RT. and the pH adjusted to 7 with dilute NaHCO<sub>3</sub> solution. The mixture was diluted with ethyl acetate and the organics separated from the aqueous fraction. The organics were washed with brine, dried over MgSO<sub>4</sub> and concentrated. The remainder was purified on silica gel column chromatography with dichloromethane and then 10% ethyl acetate/dichloromethane to give the title compound (0.13 g, 50%). R<sub>f</sub> = 0.3; <sup>1</sup>H NMR (CDCl<sub>3</sub>) δ 7.80-6.90 (m, 18 H), 3.30 (q, 2H, J=8.5 Hz), 2.10 (s broad, 1H), 0.70 (t, 3H, J=8.5 Hz) ppm.

#### **ethyl [[1-ethyl-2-4,5-diphenyl-1H-imidazole]biphenyl-3-yl]oxy]acetate (12).**

A 25 mL RB flask was charged with DMF (2.5 mL), K<sub>2</sub>CO<sub>3</sub> (0.055 g, 0.04 mmol), ethyl bromoacetate (0.038 g, 0.02 mmol) and compound **11** (0.10 g; 0.22 mmol). The biphasic mixture was stirred overnight and was diluted sequentially with ethyl acetate 15 mL and water 15 mL. The layers were separated and the organic fraction was washed with water, dried over Na<sub>2</sub>SO<sub>4</sub> and concentrated. The remainder was purified by silica gel column chromatography with ethyl acetate and hexanes as a mobile phase. A gradient elution from hexane to 25% ethyl acetate in hexane provided the title compound. (0.80 g, 70%). R<sub>f</sub> = 0.6; <sup>1</sup>H NMR (CDCl<sub>3</sub>) δ 7.90-6.90 (m, 18 H), 4.60 (s, 2H), 4.20 (q, 2H, J=7 Hz) 3.30 (q, 2H, J=9 Hz), 1.70 (t, 3H, J=7 Hz), 0.60 (t, 3H, J=9 Hz) ppm.

#### **[[1-ethyl-2-4,5-diphenyl-1H-imidazole]biphenyl-3-yl]oxy]acetic acid, sodium form (2) Inhibitor 2.**

A 25 mL RB flask was charged with ethanol (7 mL), NaOH (0.4 g, 10 mmol), compound **12** (0.10 g, 0.16 mmol) and 1 mL of water. The mixture was heated to reflux for 1 h and cooled to room temperature. The mixture was concentrated and purified on SP207 gel using a step gradient with 100 mL volumes starting with water; 10% methanol in water; 20% methanol in water; 30% methanol in water; 50% methanol in water; methanol in water; 90% methanol in water; methanol to give 0.09 g of final product. R<sub>f</sub> = 0.05; HPLC: Retention Time: 15.0 min. <sup>1</sup>H NMR (CD<sub>3</sub>OD) δ 7.90-6.90 (m, 18 H), 4.60 (s, 2H), 3.30 (q, 2H, J=9 Hz), 0.60 (t, 3H, J=9 Hz) ppm.

#### **Results and Conclusion:**

Herein we have described the preparation of two inhibitors of αP2. The methods disclosed are suitable to generate milligram to gram quantities of these inhibitors. All of the reactions are robust and give fair to excellent yields of products. A key component to the isolation of the final salts is the utilization of SP-207 resin. This resin provides a convenient system for preparative reverse phase isolation of organic salts. Herein the isolation of these fatty acid salts was demonstrated.

The synthesis of these potent inhibitors has been accomplished and it is intended that further utilization of these unique compounds will enhance our understanding of diabetes and new treatments for the disease. This rationale is consistent with the information reported by Hotamisligil utilizing the *ob/ob* mouse model. These animals suffer from severe obesity and very high glucose levels. In this animal model, the αP2 inhibitors not only reduced glucose levels but also demonstrated increased sensitivity to insulin. The Harvard results suggest that new diabetic treatments could be forthcoming by interference of the fatty acid trafficking pathway.

#### **Acknowledgements**

We would like to thank Dr. Radman Ali,<sup>14a</sup> Dr. Leroy Stagers and Clemson SC Life<sup>14b</sup> for their help and support during the course of this project.

#### **References**

1. Data taken from the American Diabetes Association Web Site 2006.
2. For a general overview of diabetes see: Cecil, *Essentials of Medicine*, 6<sup>th</sup> Ed., W B Saunders Co. An Imprint of Elsevier Inc. **2004**, 621-638.
3. Saltiel, A. R.; Olefsky, J. M.; *Diabetes*, **1996**, *45*, 1661-1669.
4. Rosenstock, J.; Schwartz, S. L.; Clark, C. M., Jr.; Park, G. D.; Donley, D. W.; Edwards, M. B. *Diabetes Care* **2001**, *24*, 631-636.
5. Gerich, J. E. *N. Eng. J. Med.* **1989**, *321*, 1231-1245.
6. Baily, C. J.; Path, M. R. C.; Turner, R. C. *N. Eng. J. Med.* **1996**, *334*, 574-579.
7. a) Magnin, D. R.; Robl, J. A.; Sulsky, R. B. Augei, D. J. et al. *J. Med. Chem.* **2004**, *47*, 2758-2598. b) Vilsboll, T. *British J. Diabetes and Vascular Disease* **2007**, *7*, 69-74. c) Pratley, R. E.; Gilbert, M. *Rev. Diabet. Stud.* **2008**, *5*(2), 73-94.
8. a) Scheja, L.; Makowski, L.; Uysal, K. T.; Wiesbrock, S. M.; Shimshak, D. R.; Meyers, D. S.; Morgan, M.; Parker, R. A.; Hotamisligil, G. S. *Diabetes* **1999**, *48*, 1987. b) Uysal K.T.; Scheja, L.; Wiesbrock S. M.; Bonner-Weir S.; Hotamisligil, G. *Endocrinology* **2000**, *141*, 3388-3342.
9. a) Banaszak, L.; Winter, N.; Xu, Z.; Bernlohr, D. A.; Cowan, S.; Jones, T. A. *Adv. Protein Chem.* **1994**, *45*, 89. b) Bernlohr, D. A.; Doering, T. L.; Kelly, T. J. Jr.; Lane, M. D. *Biochem. Biophys. Res. Commun.* **1985**, *132*, 850. c) Zimmerman, A. W.; Veerkamp, J. H. *Cellular and Molecular Life Sciences* **2002**, *59*, 1096. (d) Hertz, A.V.; Bernlohr, D. A. *Trends in Endocrinology and Metabolism*. **2000**, *11*, 175.
10. Scheja, L.; Makowski, L.; Uysal, K. T.; Wiesbrock, S. M.; Shimshak, D. R.; Meyers, D. S.; Morgan, M.; Parker, R. A.; Hotamisligil, G. S. *Diabetes* **1999**, *48*, 1987.
11. Uysal K.T.; Scheja, L.; Wiesbrock, S. M.; Bonner-Weir S.; Hotamisligil, G. *Endocrinology* **2000**, *141*, 3388-3342.
12. Furuhashi, M.; Tuncman, G.; Görgün, C. Z.; Makowski, L.; Atsumi, G.; Vaillancourt, E.; Kono, K.; Babaev, V. R.; Fazio, S.; Linton, M. F.; Sulsky, R.; Robl, J. A.; Parker, R. A.; Hotamisligil, G. S. *Nature* **2008**, *447*, 959-965.
13. a) Ringom, R.; Axen, E.; Uppenberg, J.; Lundbaeck, T.; Rondahl, L.; Barf, T. *Bioorg. Med. Chem. Lett.* **2004**, *14*, 4449-4452. b) Lehmann, F.; Haile, S.; Axen, E.; Medina, C.; Uppenberg, J.; Svensson, S.; Lundbaeck, T.; Rondahl, L.; Barf, T. *Bioorg. Med.*

- 
- Chem. Lett.* **2004**, *14*, 4445-4448. c) Sulsky, R.; Magnin, D. R.; Huang, Y.; Simpkins, L.; Taunk, P.; Patel, M.; Zhu, Y.; Stouch, T. Y.; Bassolino-Klimas, D.; Parker, R.; Harrity, T.; Stoffel, R.; Taylor, D. S.; Lavoie, T. B.; Kish, K.; Jacobson, B. L.; Sheriff, S.; Adam, L. P.; Ewing, W.; Robl, J. A. *Bioorg. Med. Chem. Lett.* **2007**, *17*, 3511-3515.
14. Robl, J. A.; Sulsky, R. B.; Magnin, D. R. U.S. Patent **2003**, #6,548,529.
  15. Generous support was provided through NSF Grant 0411383. This grant is in support of NSF HBCU-UP. b. The SC Life Project at Clemson University provided additional resources for undergraduate research. The SC LIFE Project is supported by an award to Clemson University from the Howard Hughes Medical Institute.

---

# The Effect of Incubation Time on the Generation of Benzene in Sierra Mist Free

Sarah Law

Heathwood Hall Episcopal School, 3000 S. Beltline Boulevard, Columbia, SC 29201

Received May 5, 2009

This experiment performed was to determine the effect of the length of incubation time on the generation of benzene from ascorbic acid and potassium benzoate in Sierra Mist Free. The results would provide useful information on storage methods for soda which might allow people to reduce their benzene intake from soda, thus decreasing their carcinogen accumulation and possibly lowering their risk for developing associated cancers. A headspace gas chromatography and mass spectrometry method was used for the analysis of benzene. Quantitation was preformed using Agilent Enhanced Chem Station D.01.02. A calibration curve was generated by creating dilutions of benzene in deionized water. The range of detection was between 0.52 ng/mL and 20.0 ng/mL. Each sample of Sierra Mist Free was prepared for incubation by adding 10 mL of Sierra Mist Free to a headspace vial. There were 4 samples per group. Groups 1-8 were incubated at 50 °C for a certain amount of time over a 14 day period. Group 9 was the control group, incubated at room temperature. The data showed that no benzene was generated in any sample for any given period of incubation time at 50 °C or room temperature. The hypothesis, which stated that samples incubated at for a longer time at 50 °C would generate more benzene than samples incubated at 50 °C for a shorter period of time or at room temperature, was rejected, and the null hypothesis, which stated that incubation time would have no effect on the amount of benzene generated, was accepted.

## Introduction

Anyone who indulges in Coke, Sprite, Mountain Dew, or other sodas generally recognizes the negative effects of drinking carbonated drinks: for example, the caffeine, the high sugar, the empty calories, the possibility of cavities, and so on. But it is generally thought that drinking soda in moderation can be acceptable in terms of health. Recently, however, it has come under speculation that drinking soda—particularly diet soda containing both sodium benzoate or potassium benzoate and ascorbic acid—may lead to an increased risk for associated cancers such as leukemia, (8). Sodium benzoate and potassium benzoate are both salts that occur in nature, but they are more than often produced chemically when added as preservatives in foods and beverages. They are very effective at killing bacteria, yeast, and fungi, but they only work when the pH is less than 3.6. They are most commonly ingredients in foods and drinks with a high acid content, like soda, vinegar, fruit juice, and salad dressing, (6). Ascorbic acid is more commonly known as Vitamin C, and it is found naturally in fruits and vegetables like oranges, tomatoes, strawberries, and broccoli. Humans have to consume foods with Vitamin C, because the human body does not produce it. Vitamin C is needed to carry out many chemical reactions in the body, and it also acts as an antioxidant, bonding to free radicals (atoms, molecules, or ions with unpaired electrons that are very reactive) that “might otherwise damage healthy tissue” or harm “molecules like DNA, lipids, proteins, and carbohydrates,” (5). Vitamin C is often added to foods and beverages to prevent spoilage or to add nutrients. Sodium benzoate, potassium benzoate, and ascorbic acid are not harmful by themselves, but in sodas, juice, and even flavored water, sodium benzoate or potassium benzoate can react with ascorbic acid in a metal catalyzed hydroxyl radical reaction to form benzene, (3). Herein lies the problem: “The US Department of Health and Human Services (DHHS) classifies benzene as a human carcinogen—a compound that promotes cancer,” (9).

Benzene has the chemical formula  $C_6H_6$ , and it is the simplest aromatic hydrocarbon. Only slightly soluble in water, benzene is a clear, colorless liquid with a characteristic odor that boils at 80.1°C (176.2°F) and solidifies at 5.5°C (41.9°F), (1). Although benzene does occur as an uncombined molecule, it is more threatening when it is manmade and used in industry. Benzene is often used as an industrial solvent, and it is involved in the production of rubber, plastic, detergents, dyes, and synthetic fibers, (8, 9). Prolonged exposure has been linked to the development of several different types of cancer, particularly AML leukemia, (8). People are exposed to benzene everyday from auto exhaust, industrial emission, and second hand smoke, and in reality, the amount of benzene exposure from soda and other beverages is very small. Both the US Environmental Protection Agency (EPA) and the FDA have established the “maximum allowable level (MCL) for benzene in drinking water at 5 ppb”, and, since the identification of this problem in 1990, over 200 drinks have been tested, only 10 of which have been reported to contain benzene levels exceeding 5 ppb, (2). As with many carcinogens, however, accumulation versus exposure may be the key to cancer causing effects. Over a life time, the human body comes in contact with countless carcinogens, so even if the benzene levels in one can of soda isn’t “that high” it still makes sense for an individual to attempt to reduce or eliminate his or her beverage-related benzene intake.

The basic idea for this project came from a research experiment conducted by Robert Fray and a team from Scientific Instrument Services, Inc, (7). The team tested three brands of orange sodas purchased from a local grocery store: Brand X (a diet carbonated drink), Brand Y (a non-diet carbonated drink), and Brand Z (a non-diet non-carbonated drink). Their purpose was to study the effect of heat on the formation of benzene. (Studies have shown that benzene forms more readily at higher temperatures and in bright light. Sugar has also been shown to inhibit the production of benzene.) The team determined the benzene quantity with purge and trap thermal desorption gas chromatography for separation and mass spectrometry for

analysis. Samples of each brand of orange soda were incubated at 20°C, 50°C and 90°C. See “Table 1: Benzene Levels in Soda at 20, 50, and 90°C” for their results, (7):

Sample	Purge & Trap Temperature(°C)	Benzene (pg/μl)
X	20	0.36
X	50	0.60
X	90	1.45
Y	20	0.70
Y	50	0.90
Y	90	0.14
Z	20	5.5
Z	50	7.4
Z	90	10.1

Table 1: Benzene levels in soda at 20, 50 and 90°C

After observing the data, the team concluded that there is a “definite trend towards higher benzene levels found in these beverages as the incubation temperature is increased,” (7). The exception was Brand Y incubated at 90°C. The team said this error was most likely a result of some difficulties they had in keeping the lid on the flask when Brand Y, which was found to be more carbonated than Brand X and Z, was heated to 90°C. The pressure produced from Brand Y at that heat level kept making the lid pop off.

The experiment to be conducted for this project is different from the experiment conducted by Robert Fray’s team. Only one brand of soda will be used. The soda used in this experiment will be Sierra Mist Free because it contains both ascorbic acid and potassium benzoate, has no sugar, and because the FDA has previously detected benzene in Sierra Mist Free. A headspace gas chromatography and mass spectrometry method will be used for analysis of benzene in this experiment. According to Henry’s Law, “the solubility (C) of a gas or volatile substance in a liquid is proportional to the partial pressure (P) of the substance over the liquid,” (10). In mathematical terms, Henry’s law can be stated as:

$$P=kC$$

where k is a constant called “Henry’s law constant and it is characteristic of the solvent and the solute, (10). The amount of benzene dissolved in each sample of Sierra Mist Free can be determined by analyzing a sample of headspace gas from each of the headspace-vials containing Sierra Mist Free. The headspace sampler will remove a sample of gas from each of the headspace vials, and then a gas chromatography will be used to separate the benzene and internal standard. Finally, a mass spectrometer will be used to detect and quantify the amount of benzene present, (4). The purpose will be to determine the effect of incubation time on

the amount of benzene formed at 50°C over a period of 14 days. The data found in this experiment will be useful information regarding how people can reduce their benzene intake from soda, thus decreasing their carcinogen accumulation and possibly lowering their risk for developing leukemia. It is hypothesized that the amount of benzene detected in Sierra Mist Free samples incubated at 50°C for a longer period of time will be higher than the amount of benzene detected in samples incubated at 50°C for a shorter period of time or in samples incubated at room temperature. The null hypothesis is that there will be no difference in the amount of benzene detected in samples of Sierra Mist Free that were incubated at 50 °C or at room temperature for different periods of time.

## Materials and Methods

This experiment was conducted at the Toxicology lab of the South Carolina Enforcement Division, using cans of Sierra Mist Free obtained from a local grocery store, 99% pure benzene (Fisher Scientific), tert-butanol HPLC-grade (Aldrich Chemical Company), methanol (Fisher Scientific), and deionized water. Safety goggles and gloves were worn at all times, and a fume hood was used during the preparation of stock solutions and calibrators to limit exposure to benzene fumes. An Agilent Technologies G1888 Headspace Sampler, 6890N Gas Chromatographer, and 5973N Mass Selective Detector were used to process the samples

First, a 1 mg/mL stock solution of benzene in methanol was prepared. Approximately 80 mL of methanol was added to a 100 mL volumetric flask. Considering that the benzene was only 99% pure and knowing that the density of benzene is 0.88 g/mL, it was calculated that 115 μL of 99% pure benzene would be needed to create the stock solution. A micropipeter was used to add 115 μL of 99% pure benzene to the volumetric flask, and then the solution was QS-ed to 100 mL with methanol. Second, a 1 ng/mL working standard was prepared by creating a 1/1000 dilution of the stock solution in deionized water: 100 μL of the stock solution was diluted in 100 mL of deionized water. Third, the calibrators were created by diluting specific amounts of the working standard in 25 mL of deionized water: 13 μL of working standard were added to 25 mL of water to create a 0.52 ng/mL calibrator, 25 μL of working standard were added to 25mL of water to create a 1.0 ng/mL calibrator, 50 μL of working standard were added to 25 mL of water to create a 2.0 ng/mL calibrator, 125 μL of working standard were added to 25 mL of water to create a 5.0 ng/mL calibrator, 250 μL of working standard were added to 25 mL of water to create a 10.0 ng/mL calibrator, and 500 μL of working standard were added to 25 mL of water to create a 20.0 ng/mL calibrator. The positive control was a 10 ng/mL solution of working standard in deionized water, and the negative control was 10 mL of deionized water. As an internal standard, 50 μL of 0.01% tert-butanol was added to each calibrator.

36 samples of Sierra Mist Free were prepared by adding 10 mL of Sierra Mist to headspace vials, and then the vials were sealed. The 36 samples were divided into 9 groups of 4. 32 of the samples (Groups 1-8) went into a headspace oven at 1:00 pm on December 31, 2008 to incubate at 50°C. Group 9 was a control group. Group 1 was removed from the oven at

1:00pm on the following day (January 1, 2009), and those samples were allowed to cool back down to room temperature. The same procedure was repeated for all the samples in Groups 2-7. Group 8 was allowed to incubate for 14 days.

Group #	# of Days in Oven
1	1
2	2
3	3
4	4
5	5
6	6
7	7
8	14
9	0

Table 2: Length of Incubation for soda samples in groups 1-9.

Prior to analysis 50 µL of internal standard was added to each sample with a syringe. Then the samples and calibrators were loaded into the autosampler for analysis. Finally, quantitation was performed using Agilent Enhanced Chem Station D.01.02.

## Results

No statistical analysis was run.

Calibrator Concentration (ng/mL)	Response
20.0	49841
10.0	30781
5.00	14188
2.00	4770
1.00	2951
0.52	1170

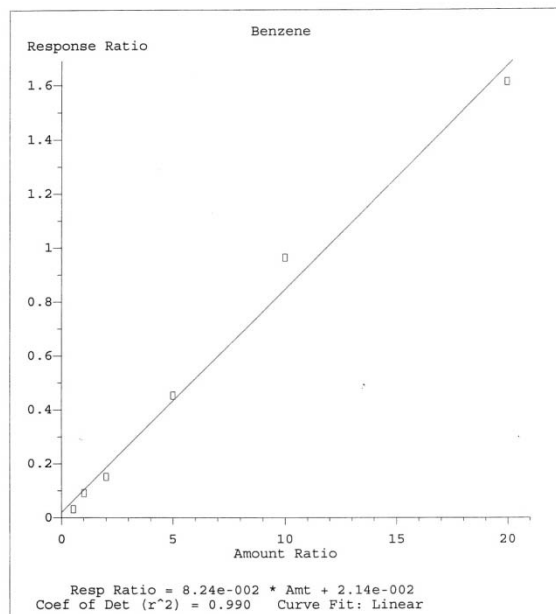
Table 3: The benzene response from each calibrator

Control	Response
Positive Control (10ng/mL)	30931
Negative Control	0

Table 4: The Benzene Response from the Positive and Negative Controls

	0	1	2	3	4	5	6	7	14
1	0	0	0	0	0	0	0	0	0
2	0	0	0	0	0	0	0	0	0
3	0	0	0	0	0	0	0	0	0
4	0	0	0	0	0	0	0	0	0

Table 5: The Benzene Response for Samples of Sierra Mist Free Over Time. Down: Headspace Vial Sample Number. Across: Number of Days of Incubation.



Method Name: C:\MSDCHEM\1\METHODS\BENZENE1.M  
Calibration Table Last Updated: Mon Jan 19 12:55:52 2009

Graph 1: Calibration curve

## Discussion

The data in Table 3: The Benzene Response from Each Calibrator shows that HS/GC/MS can be used to detect and quantify benzene. This data was used to create the calibration curve seen in Graph 1: Calibration Curve. The range of detection was 0.52 ng/mL to 20.0 ng/mL. The data in Table 4: The Benzene Response from the Positive and Negative Controls shows that the HS/GC/MS was working properly.

The purpose of this project was to determine the effect of incubation time over a period of 14 days on the generation of benzene from the ascorbic acid and potassium benzoate in Sierra Mist Free. It was hypothesized that the amount of benzene detected in Sierra Mist Free samples incubated at 50°C for a longer period of time would be higher than the amount of benzene detected in samples incubated at 50°C for a shorter period of time or in samples incubated at room temperature. The null hypothesis was that there would be no difference in the amount of benzene detected in samples of Sierra Mist Free that were incubated at 50 °C or at room temperature for different periods of time. The data in Table 5: The Benzene Response for

---

Samples of Sierra Mist Free Samples Over Time shows that no benzene was detected in any sample for any period of incubation at any incubation temperature. Therefore, the hypothesis must be rejected and the null hypothesis must be accepted. With such data it was neither possible nor necessary to run statistical analysis.

There are several possible sources of error. Because the limit of detection achieved by the lowest calibrator was 0.52 ng/mL, trace levels of benzene below 0.52 ng/mL may have gone undetected. Another possibility is that the aluminum can is in some way involved in the generation of benzene from ascorbic acid and potassium benzoate in soda. Samples in this experiment were not incubated in aluminum cans; the samples were incubated in glass vials because the aluminum cans burst when incubated at 50 °C in the headspace oven. A third possibility is that the carbonation in soda plays a roll in the generation of benzene. The can from which all of the samples of Sierra Mist Free were obtained was allowed to sit open for 1 hour to go flat because pipeting an accurate amount of sample was not possible when the drink was first open due to air bubbles created in the pipet from the carbonation. Further research might involve creating a lower limit of detection or finding successful methods for incubating aluminum cans or pipeting carbonated soda samples. Also, other brands of soda might be tested for comparison.

## Acknowledgements

I would like to thank Robert Sears for all of his help and advice and for generously giving time to teach and supervise my procedure. I would also like to thank the South Carolina Law Enforcement Division for allowing me to conduct my experiment at their toxicology lab.

## References

1. "Benzene." *Britannica*. 2000.
2. U.S Food and Drug Administration. "Questions and Answers on the Occurrence of Benzene in Soft Drinks and Other Beverages." 12 July 2007. Web. 30 Nov. 2008
3. Production of Benzene from Ascorbic Acid and Sodium Benzoate. Manhattan, Kansas: AIB International, 2006. (PDF version of document downloaded 30 Nov. 2008).
4. Clark, Jim. "The Mass Spectrometer." 2000. 30 Nov. 2008 <<http://www.chemguid e.co.uk/analysis/masspec/howitworks.html>>
5. Ellis-Christensen, Tricia. "What is Ascorbic Acid?" wiseGEEK. 27 Sept. 2008 <<http://www.wisegeek.com/what-is-ascorbic-acid.htm>>
6. Ellis-Christensen, Tricia. "What is Sodium Benzoate?" wiseGEEK. 27 Sept. 2008 <<http://www.wisegeek.com/what-is-sodium-benzoate.htm>>
7. Fray, Robert. "Detection of Benzene in Carbonated Beverages with Purge & Trap Thermal Desorption GC/MS." Scientific Instrument Services, Inc. 2008. Web. 27 Sept. 2008.
8. Nordqvist, Christian. "High Benzene Levels Found in Some Soft Drinks." Medical News Today. 20 May 2006. 27 Sept 2008 <<http://www.medicalnewstoday.com/articles/43763.php>>
9. Pilon, Brad. "Diet Pop- Do You REALLY Know Enough?" The Nutrition Help Blog. 29 Nov. 2006. 27 Sept. 2008 <<http://nutritionhelp.blogspot.com/2006/11/diet-pop-do-you-really-know-enough-you.html>>
10. Senese, Fred. "Henry's Law." General Chemistry Glossary. 2001. Web. 8 Feb 2009.

---

# Effect of Thaw Temperature on Murine Blastocyst Development

Heather M. Barton<sup>a</sup>, H. Lee Higdon III, Ph.D.<sup>b</sup>, Jennifer E. Graves-Herring, M.S.<sup>b</sup>, William R. Boone, Ph.D.<sup>b</sup>

<sup>a</sup>Department of Animal and Veterinary Sciences, Clemson University, Clemson, SC

<sup>b</sup>Department of Obstetrics and Gynecology, Greenville Hospital System University Medical Center, Greenville, SC

Received June 5, 2009

Assisted Reproductive Technology (ART) methods are employed to help infertile couples conceive. One such ART procedure is in vitro fertilization (IVF) and embryo culture (EC). During IVF-EC, supernumerary embryos are often produced and cryopreserved for future use. Embryos frozen and thawed have reduced rates of blastocyst development. Thawing temperature is one of the factors thought to affect embryo development after cryopreservation. The objective of this study was to determine if varying thaw temperatures affect embryo development. Using a randomized, controlled study, approximately 230 two-cell murine embryos were exposed to cryoprotectants and cryopreserved in lots of 15 embryos per straw. A total of 16 straws were cryopreserved. Cryopreserved embryos were thawed in water baths set at either 30°C (n = eight straws) or 37°C (n = eight straws). Once the straws were thawed and the cryoprotectant removed, the embryos were incubated for 72 hours and assessed for blastocyst development. Proportions between blastocyst developments were analyzed using the Chi square test. Blastocyst development for straws thawed at 30°C was 52.1% (63/121) compared to 45.5% (50/110) for straws thawed at 37°C. These values were not significantly different ( $P = 0.4$ ). In conclusion, the range of thaw temperature used for this study had no effect on post-thaw embryo development. Future studies should assess other aspects of the thawing procedure, including length of time straws remain in the water bath, as well as the effect of pre-thawing straws at room temperature before placing them in the water bath.

## Introduction

For three decades, Assisted Reproductive Technology (ART) has been helping infertile couples conceive. Since the birth of the first “test-tube baby” in 1978, reproductive technology has made many advances in its ability to overcome infertility (Sher et al., 2005). Couples are classified “infertile” if they have not used contraception for a year or more and have not conceived. In 2004, nearly 50,000 infants were born in the United States to “infertile” couples because of ART (Centers for Disease Control and Prevention, 2006).

An in vitro fertilization (IVF) and embryo culture (EC) cycle begins when a woman starts taking fertility drugs or has her ovaries monitored for follicular development (Wright et al., 2004; Centers for Disease Control and Prevention, 2006). The next step is egg-retrieval, after which the eggs (oocytes) are combined with sperm in the laboratory. The subsequent embryos are evaluated morphologically and two to three of the “best” embryos are transferred to the patient. If the transfer is successful and implantation occurs, the cycle is deemed a clinical pregnancy. The last step, and ultimate goal, is a live-birth delivery, defined as a birth resulting in one or more live born neonates (American Society for Reproductive Medicine, 2004). The Center for Disease Control and Prevention reported that of the 127,977 IVF-EC cycles initiated in 2004, 36,760 (28.7%) resulted in live-birth deliveries.

In many cases, infertile women have to undergo multiple cycles before pregnancy is established, and even more cycles before a live-birth is obtained. Often times, with more cycles initiated comes an increase in number of

embryos placed back into the uterus. This increased number of embryos transferred often translates into a multiple pregnancy. Unfortunately, multiple pregnancy often leads to serious consequences, especially if the pregnancy results in triplet births or greater. Therefore, multiple-infant pregnancies should be considered a complication of ART, as they are associated with a number of problems including higher rates of caesarean section, prematurity, low birth weight, and infant disability or death. Nearly one-third of pregnancies resulting from ART conclude in multiple-infant live births.

Distributing the embryos obtained during the course of one IVF-EC cycle over a number of cycles is a beneficial alternative to undergoing fresh retrievals each time (Edgar et al., 2000). Cryopreserving the embryos from the first cycle and using them for later cycles fully uses the potential of the first oocyte retrieval, while allowing all the embryos resulting from that cycle to be used rather than discarded (Jones et al., 1997; Schnorr et al., 2000; Edgar et al., 2005). Cryopreserving also provides a useful tool for avoiding multiple-infant pregnancies. Instead of transferring numerous embryos in the first transfer, some may be stored for another transfer, thus reducing the risk of multiple infants (Oehninger et al., 2000; Cohen et al., 2001) and increasing the probability of obtaining a pregnancy with one ART cycle (Jones et al., 1997).

Another complication with the IVF-EC cycle is ovarian hyperstimulation syndrome (OHSS), and occurs in an estimated 1% to 10% of ART cases when the ovaries are stimulated for ovulation induction (Fasouliotis and Schenker, 2005). In extreme cases, OHSS can cause severe

---

morbidity and even death. If the woman fails to conceive, the symptoms disappear rapidly; however, if a pregnancy is obtained, the symptoms may become progressively worse (Sher et al., 2005). According to Chung et al. (2006) and Edgar et al. (2005), OHSS is a greater risk in multiple-infant pregnancies and because of this, it is recommended that patients with severe OHSS undergo oocyte collection, cryopreserve of their embryos, and end the cycle, postponing embryo transfer until later.

These complications associated with the ART process (the need for numerous cycles to obtain a pregnancy, multiple-infant pregnancies, and the risks of OHSS) have been decreased by the growing use of cryopreservation in ART laboratories (Edgar et al., 2000; Oehninger et al., 2000; Schnorr et al., 2000; Edgar et al., 2005).

Cryopreservation is the preservation of cells, tissues, organs, or embryos by freezing. Since the early 1980's, ART has utilized this technology as a means to store embryos for future use (Trounson and Mohr, 1983). The implementation of cryopreservation has given ART clinics the freedom to use fewer embryos for transfer, as they are able to store the supernumerary embryos and use them later if pregnancy is not established (Edgar et al., 2005). Freezing provides an alternative for patients who may not wish to discard unused embryos, but who are also wary of a multiple-infant pregnancy and so do not wish to transfer all the embryos at once.

Even though cryopreservation is advantageous for patients, it has its own drawbacks. The 2005 National Summary of ART clinics in the United States reported that the percentage of transfers resulting in live births from fresh embryos in women under 35 years of age was about 43%, while only 32% of thawed embryos resulted in live births (Society for Assisted Reproductive Technology, 2006). However, some believe that the strict criteria used to choose fresh embryos for transfer gives an advantage to those embryos and, consequently, a disadvantage to those embryos left for cryopreservation (Edgar et al., 2000).

Edgar et al. (2000) found that nearly 45% of thawed embryos suffered some amount of blastomere (cell) loss, causing an approximate 30% reduction in implantation. They also suggested from these data that 80% of the resulting implantations arise from thawed embryos, which suffered no blastomere loss. Therefore, if methods can be altered in such a way as to protect the blastomeres from damage during cryopreservation/thawing, the patient should have an improved chance for implantation with the thawed embryos.

The purpose of this study was to determine if varying the temperatures at which cryopreserved embryos are thawed affects the rate of post-thaw blastocyst development.

## Materials and Methods

### Animals

The complete cryopreservation procedure for mouse embryos has been described earlier (Boone et al, 2004). Specific pathogen-free mice (B6C3F1) were obtained from Jackson Labs. Female mice were superovulated with intraperitoneal injection of 5.0 International Units (IU) of pregnant mare's serum gonadotropin (PMSG; Calbiochem, San Diego, CA). Each female was injected intraperitoneally with 5.0 IU human chorionic gonadotropin (hCG; Sigma Aldrich, St. Louis, MO) 48 hours after PMSG injection and immediately placed with a male. Females were sacrificed approximately 43 hours after hCG injection. Embryos were collected via oviductal lavage using approximately 0.1 mL of Dulbecco's phosphate-buffered saline. Only morphologically normal two-cell embryos were used in the study. All of these procedures complied with an approved Animal Research Committee protocol.

### Cryopreservation

Embryos were cryopreserved in 1.5M propanediol and 0.1M Sucrose (SAGE In-Vitro Fertilization, Inc., Trumbull, CT), and subsequently frozen at the two-cell stage of development using the Sage Embryo Freeze protocol. Embryos were moved through three increasing levels of cryoprotectant to help remove water from the cells. Fifteen embryos were loaded into a plastic straw and heat sealed. A total of 16 straws were used in this experiment. Next, the straws were placed in a programmable freezer (Planer Freezer, Planer Co., UK) and cooled using the following settings: Ramp 1) 23°C to -6°C at minus 2°C per minute; Ramp 2) held at -6°C for 15 minutes for seeding (seeded 5 minutes into the ramp with 10 minutes post-seeding soak); Ramp 3) -6°C to -35°C at minus 0.3°C per minute; Ramp 4) held for 5 minutes; Ramp 5) -35°C to -180°C at minus 50°C per minute; and Ramp 6) held at -180°C for 5 minutes. The straws then were removed from the freezing chamber and plunged into liquid nitrogen for storage.

### Thaw Procedure

Cryopreserved straws were thawed individually. Each was removed from the liquid nitrogen tank and allowed to thaw for 30 seconds at room temperature. The straw then was placed in a water bath for 30 seconds. Eight straws were thawed in water baths set at 30°C, and eight straws were thawed in water baths set at 37°C. Cryoprotectant was removed by exposing the embryos to decreasing concentrations of cryoprotectant (Quinn's Advantage Thaw Kit, SAGE In-Vitro Fertilization, Inc., Trumbull, CT). Upon removal of the cryoprotectants, the embryos were incubated for 72 hours and assessed for blastocyst development based on morphology.

## Statistics

Proportions between blastocyst development for the embryos in the two different thaw temperatures were analyzed using the Chi square test.

## Results

Blastocyst development for straws thawed at 30°C was 52.1% (63/121), compared with 45.5% (50/110) for straws thawed at 37°C. These two developmental rates were not statistically different ( $P = 0.4$ ). Data are depicted in Table 1.

Figure 1 shows four embryos thawed in the course of this study. Embryo A is a blastocyst, characterized by the intact zona pellucida. Embryo B is an early blastocyst that has an extruded degenerated blastomere. Embryo C is a morula containing degenerated blastomeres. Embryo D is a degenerated four-cell embryo. This figure represents the type of embryos observed in this project. For our data, two of these embryos were classified as blastocysts and two as non-blastocysts.

Thaw Temperature (°C)	Non-blastocyst (%)	Blastocyst (%)	P value
30	47.9 (58/121)	52.1 (63/121)	0.4
37	54.5 (60/110)	45.5 (50/110)	

Table 1. Percent of post-thaw mouse blastocyst development after thawing in different temperatures.

## Discussion

Cryopreservation has been a useful tool for infertile couples undergoing IVF-EC. However, thawed embryos have reduced rates of blastocyst development which adversely affects birth rates. The objective of this study was to assess the effect of different thaw temperatures on post-thaw blastocyst development.

Thaw procedures reported in other studies differ considerably. Valojerdi et al. (2002) reported thawing two-cell mouse embryos for 10 seconds at room temperature before shaking them in a 20°C water bath for 20 seconds and subsequently passing them through a series of dilution and rehydration steps. Another study reported thawing the

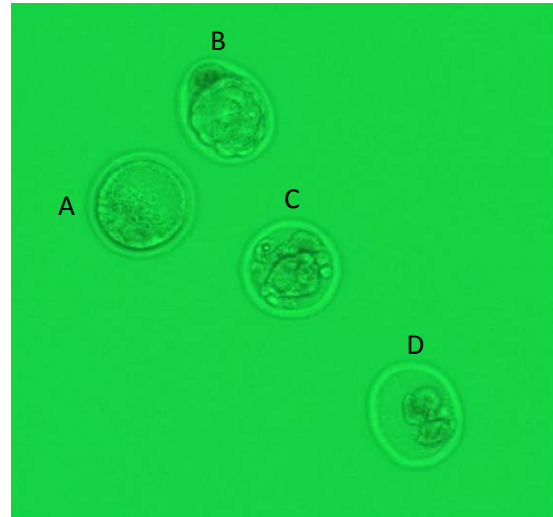


Figure 1. Development of four murine embryos 72 hours post-thaw.

vials in which the embryos were stored in a water bath at 31°C for 3 minutes before moving the embryos through a series of dilutions to remove the cryoprotectants (Burns et al., 1999). These two examples demonstrate how diverse the procedures are for thawing cryopreserved embryos, with a time difference of over two-and-one-half minutes and a temperature difference of 11°C.

For our study, murine embryos were cryopreserved and sequentially thawed in water baths at 30°C or 37°C for 30 seconds. Our results determined no significant difference in post-thaw murine blastocyst development between embryos thawed at 30°C and those thawed at 37°C. This may provide evidence to suggest that slightly varying thaw temperatures are inconsequential to the development of post-thaw blastocysts. However, many other aspects of the cryopreservation process should be assessed to determine their roles in affecting thawed-embryo development. For example, just as the time and temperature of reported thaw procedures varied, so do the dilution and rehydration steps. Perhaps if more accurate and precise methods can be developed for thawing cryopreserved embryos, subsequent thawed-embryo development rates, and ultimately birth rates, can be improved.

## References

1. American Society for Reproductive Medicine (ASRM). 2004. Assisted Reproductive Technology in the United States: 2000 results generated from the American Society for Reproductive Medicine/Society for Assisted Reproductive Technology Registry. *Fertility and Sterility*. Vol. 81, No.5: 1207 – 1220.
2. Boone W.R., J.E. Johnson, D.W. Blackhurst, and H.L. Higdon III. 2004. Cryopreservation methodologies: freezing location and protocol alter development of mouse embryos. *Contemporary Topics*. Vol. 43: 26 – 31.
3. Burns, W.N., T.W. Gaudet, M.B. Martin, Y.R. Leal, H. Schoen, C.A. Eddy, and R.S. Schenken. 1999. Survival of cryopreservation and thawing with all blastomeres intact

- 
- identifies multicell embryos with superior frozen embryo transfer outcome. *Fertility and Sterility*. Vol. 72, No. 3: 527 – 532.
4. Centers for Disease Control and Prevention (CDC). 2006. 2004 Assisted Reproductive Technology Success Rates: National Summary and Fertility Clinic Reports.
  5. Chandra A, G.M. Martinez, M.D. Mosher, J.C. Abma, and J. Jones. 2005. Fertility, family planning, and reproductive health of U.S. women: Data from the 2002 National Survey of Family Growth. National Center for Health Statistics. *Vital Health Stat* Vol. 23, No.25.
  6. Chung, K., C. Coutifaris, R. Chalian, K. Lin, S. Ratcliffe, A.J. Castelbaum, M.F. Freedman, and K.T. Barnhart. 2006. Factors influencing adverse perinatal outcomes in pregnancies achieved through use of in vitro fertilization. *Fertility and Sterility*. Vol. 86, No. 6: 1634 – 1641.
  7. Cohen, J, and H.W. Jones Jr. 2001. How to avoid multiple pregnancies in assistive reproductive technologies. *Seminars in Reproductive Medicine*. Vol. 19, No. 3: 269 – 278.
  8. Edgar, D.H., H. Bourne, H. Jericho, and J.C. McBain. 2000. The developmental potential of cryopreserved human embryos. *Molecular and Cellular Endocrinology*. Vol. 169: 69 – 72.
  9. Edgar, D.H., J. Archer, and H. Bourne. 2005. The application and impact of cryopreservation of early cleavage stage embryos in assisted reproduction. *Human Fertility*. Vol. 8, No. 4: 225 – 230.
  10. Fasouliotis, S. J., and J.G. Schenker. 2002. Failures in assisted reproductive technology: an overview. *European Journal of Obstetrics & Gynecology and Reproductive Biology* Vol. 107: 4 – 18.
  11. Jones, H.W., H.J. Out, E.H. Hooman, S.G. Driessen, and H.J. Bennink. 1997. Cryopreservation: the practicalities of evaluation. *Human Reproduction*. Vol. 12, No. 7: 1522 – 1524.
  12. Lassalle, B., J. Testart, and J.P. Renard, 1985. Human embryo features that influence the success of cryopreservation with the use of 1,2-propanediol. *Fertility and Sterility*. Vol. 44, No. 5: 645 – 651.
  13. Nagy A, M. Gertsenstein, K. Vintersten, and R. Behringer. 2003. Manipulating the mouse embryo. A laboratory manual. Cold Spring Harbor Laboratory Press. Cold Spring Harbor, NY.
  14. Niemann, H. and B. Reichelt. 1993. Manipulating early pig embryos. *Journal of Reproduction and Fertility*. [Supplement] Vol. 48; 75 – 94.
  15. Oehninger, S., J. Mayer, and S. Muasher. 2000. Impact of different clinical variables on pregnancy outcome following embryo cryopreservation. *Molecular and Cellular Endocrinology*. Vol 169: 73 – 77.
  16. Queenan, J.T., L.L. Veeck, J.P. Toner, S Oehninger, and S.J. Muasher. 1997. Cryopreservation of all prezygotes in patients at risk of severe hyperstimulation does not eliminate the syndrome, but the chances of pregnancy are excellent with subsequent frozen-thaw transfers. *Human Reproduction*. Vol. 12, No. 7: 1573 – 1576.
  17. Schnorr, J.A., S.J. Muasher, and H.W. Jones Jr. 2000. Evaluation of the clinical efficacy of embryo cryopreservation. *Molecular and Cellular Endocrinology*. Vol. 169: 85 – 89.
  18. Senger, P.L. 2005. Pathways to Pregnancy and Parturition. 2<sup>nd</sup> Edition. Current Conceptions, Inc. Pullman, WA. 285 – 289, 348 – 365.
  19. Sher, G., V.M. Davis, and J. Stoess. 2005. In Vitro Fertilization: The A.R.T. of Making Babies. 3<sup>rd</sup> Edition. Checkmark Books. New York, NY. 63 – 65.
  20. Society for Assisted Reproductive Technology. 2006. IVF Success Rate Reports. [www.sart.org](http://www.sart.org).
  21. Trounson, A. and L. Mohr. 1983. Human pregnancy following cryopreservation, thawing and transfer of an eight-cell embryo. *Nature*. Vol. 305, No. 5936: 707 – 709.
  22. Valojerdi, M.R., M. Movahedin, and A. Hosseini. 2002. Improvement of Development of Vitriified Two-Cell Mouse Embryos by Vero Cell Culture. *Journal of Assisted Reproduction and Genetics*. Vol. 19, No. 1: 31 – 38.
  23. Wright, V.C, J. Chang, G. Jeng, and M. Macaluso. 2006. Assisted Reproductive Technology Surveillance – United States, 2003. National Center for Chronic Disease Prevention and Health Promotion (CDC). *Surveillance Summaries*. Vol. 55, No. SS04: 1-22.
-

---

# Downregulation of HIV-1 *vif* by a hammerhead ribozyme expressed from a retroviral vector

Hendley, Audrey M.<sup>a</sup> and William Jackson<sup>\*b</sup>

<sup>a</sup> Johns Hopkins University, Baltimore, MD, USA. E-mail: ahendle1@jhmi.edu

<sup>b</sup> Department of Biology and Geology, University of South Carolina Aiken, 471 University Parkway, Aiken, SC, USA. Fax: 803-641-3251; Tel: 803-641-3601; E-mail: billj@usca.edu.

Received September 1, 2009

HIV infection of CD4<sup>+</sup> T helper cells results in a gradual deterioration of immune function and leads to the onset of the Acquired Immune Deficiency Syndrome (AIDS). Current research suggests that HIV infection may be combated with ribozyme therapy. Hammerhead ribozymes are small, catalytic RNAs that can be designed to cleave substrate RNAs at specific sequences, and those targeted to HIV-1 mRNAs have been shown to greatly reduce or inhibit viral replication. The HIV-1 *virion infectivity factor* (*vif*) gene encodes a protein that counteracts an innate, antiretroviral defense mechanism of non-permissive CD4<sup>+</sup> T helper cells. This mechanism is mediated by apolipoprotein B mRNA-editing enzyme-catalytic polypeptide-like 3G (APOBEC3G), a cellular cytidine deaminase that is encapsulated into assembling virions in the absence of *vif* and is inhibitory during the next round of viral replication. *Vif* neutralizes APOBEC3G by reducing its translation and by rapid degradation of the native protein. *Vif* mRNA, therefore, may be a good target for ribozyme mediated inhibition of HIV-1 replication. To test this hypothesis a catalytic hammerhead ribozyme targeted to nucleotide 5113 of the HIV-1 genomic clone NL43 (Accession # M19221) was designed and synthesized. A non-catalytic control, *Vif*5113Δ was also designed and synthesized. *Vif*5113 and *Vif*5113Δ were cloned into the retroviral vector, pSuper.retro.puro (pSRP) to facilitate tissue culture studies. In this study, *Vif*5113 and *Vif*113Δ ribozymes were analyzed for their ability to reduce *vif* expression in an intracellular cleavage assay. These studies, as determined by Western blot analysis, suggested that *vif* expression was reduced in the presence of the catalytic ribozyme *Vif*5113.

## Introduction

HIV-1 is a retrovirus that infects CD4<sup>+</sup> T helper cells (1;2) resulting in a gradual deterioration of immune function and eventually leading to the onset of the Acquired Immune Deficiency Syndrome (3-6). In December 2007, the World Health UNAIDS Organization estimated that 33 million people worldwide were living with HIV/AIDS. It was also estimated that 14,000 people worldwide become newly infected with the Human Immunodeficiency Virus (HIV) every day (7).

The HIV-1 genome encodes nine viral genes from which fifteen functional gene products are expressed (8). One of these genes, the *virion infectivity factor* (*vif*) encodes a 23 kD protein that counteracts an innate, antiretroviral defense mechanism of CD4<sup>+</sup> T helper cells (9), the primary target of HIV (2). This resistance to HIV infection is due to the expression of APOBEC3G (human apolipoprotein B mRNA-editing enzyme catalytic polypeptide-like 3G), which acts to inhibit reverse transcription of retroviruses (8).

APOBEC3G expression is stimulated by certain viral proteins such as HIV-1 *Vif*. Normally, APOBEC3G is encapsulated into progeny virions, where it remains non-functional until the virion infects its host cell. Upon infection of the host cell and reverse transcription of the viral genome, APOBEC3G induces hypermutation from C to U in the minus strand of viral DNA resulting in G to A mutations in the positive sense DNA strand. These mutations in the viral genome inhibit normal expression of viral genes and render the target cell incapable of producing progeny virions and facilitating a productive infection (8).

*Vif* counteracts this activity by binding APOBEC3G and targeting the protein for degradation through the ubiquitin pathway (10). We hypothesized that downregulating *vif*

expression in infected cells would reconstitute the normal antiviral activity of APOBEC3G. Previous research suggested that HIV infection may be combated with ribozyme therapy (11-13). Hammerhead ribozymes are small, catalytic RNAs that can be designed to target and cleave substrate RNAs at sequence specific sites (14). These ribozymes cleave mRNAs at the target sequence XUX' where X is A, C, G, or U and X' is A, C, or U (15). In this report, a hammerhead ribozyme targeted to HIV-1 *vif* was designed and cloned into the retroviral vector, pSuper.retro.puro (16;17). This vector was chosen due to its ability to express siRNAs from the RNA Polymerase III H1 promoter, and we hypothesized that it would also efficiently express ribozymes. As a control, a non-catalytic ribozyme targeted to the same HIV-1 *vif* sequence was designed and cloned. These constructs were tested for their antiviral activity in a *vif* inhibition assay. These results suggested that *vif* expression was reduced in the presence of a hammerhead ribozyme.

## Materials and Methods

### Cloning

The HIV-1 NL43 *vif* sequence (Accession number M19921) was analyzed for the presence of potential hammerhead cleavage sites (15). One such sequence, a pGUA was located at nucleotide 5113. This sequence along with its immediate flanking sequences were used to generate a hammerhead ribozyme according to the Haseloff and Gerlach model (14). A non-catalytic control ribozyme was generated by an A to G substitution within the ribozyme catalytic core (12) (Figure 1).



70mA for 2 hours. The membrane was immediately incubated in Ponceau Stain (0.5 g Ponceau-S in 1 % acetic acid) for 5 minutes and subsequently incubated with Ponceau destain (1 % acetic acid) until the bands were visible.

### Western Blot

The membrane was blocked in PBS/5% powdered milk overnight at 4°C. The following day, the membrane was washed 2X with PBS for 2 minutes per wash, and incubated in 10 mL PBS containing 20 µg anti-FLAG M2 antibody (Stratagene) at room temperature with gentle rocking for one hour. This was followed by two washes with PBS for 2 minutes per wash. The secondary goat anti-mouse HRP conjugate antibody (Chemicon) was diluted 1:5000 in blocking solution and added to the membrane. The membrane was incubated with the secondary antibody for two hours at room temperature with gentle rocking, and then washed 3X with PBS for 5 minutes per wash. The ECL detection reagent (Amersham) was prepared and added to the membrane. The membrane was incubated at room temperature for 5 minutes, excess reagent was drained away, and the membrane was wrapped in plastic. The blot was placed in a cassette with X-ray film (Kodak) and allowed to expose the film overnight. The film was hand developed using Kodak reagents.

### Results

The HIV-1 NL43 *vif* genomic sequence was analyzed for the presence of potential hammerhead ribozyme target sites. One site, a pGUC located at nucleotide 5113 was used to design an anti-*vif* hammerhead ribozyme. This ribozyme and its non-catalytic control (Figure 1) were synthesized and cloned into the retroviral vector, pSuper.retro.puro. Sequencing was used to verify the ribozyme sequence in the resulting plasmids: pSRP5113 and pSRP5113Δ (Figure 2).

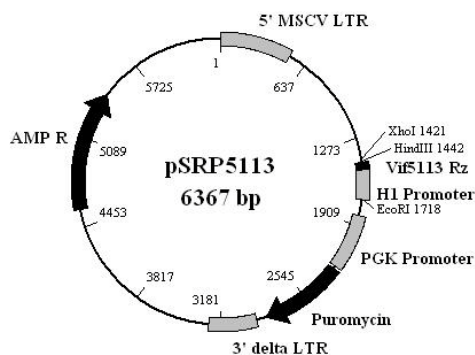


Figure 2. The retroviral vector pSRP5113. An anti-*vif* ribozyme targeted to nucleotide 5113 of the HIV NL43 sequence was cloned into the retroviral vector, pSuper.retro.puro. The resulting vector is shown. A similar vector was constructed that expresses a non-catalytic form of the ribozyme, pSRP5113Δ.

The ability of the Vif5113 hammerhead ribozyme to reduce expression was analyzed using a *vif* inhibition assay. For this, two series of co-transfections were carried out in 293T cells using either pSRP5113 or pSRP5113Δ and the HIV *vif* expression plasmid, pCMV-VifFLAG. The first series of co-transfections included 5 µg of pSRPVif5113 or pSRP5113Δ and 5 µg of pCMV-VifFLAG. A second series of co-transfections included

10 µg of either pSRPVif5113 or pSRPVif5113Δ and 5 µg of pCMV-VifFLAG. A 5 µg transfection of a GFP-expressing plasmid served as a negative control.

The intracellular cleavage ability of the anti-*vif* ribozyme was analyzed by Western blot. Forty-eight hours after each transfection series, total protein was obtained from the cells and 50 µg of each was separated using a 12% polyacrylamide gel. The separated proteins were transferred to a PVDF membrane and probed using an anti-FLAG antibody. The resulting blot was analyzed to determine the relative levels of *vif* expression. A band present at 23 kD was assumed to be HIV Vif (Figure 3).

Con(-)    1            2            3            4

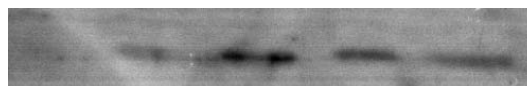


Figure 3. Analysis of *vif* expression. 293T cells were transfected as follows: Con(-) – GFP; lane 1 – 1:1 pSRPVif5113 to pCMV-VifFLAG; lane 2 – 1:1 pSRPVif5113Δ to pCMV-VifFLAG; lane 3 – 2:1 pSRP5113 to pCMV-VifFLAG; and lane 4 – 2:1 pSRP5113Δ to pCMV-VifFLAG. These results indicated that at the 1:1 ratio, the catalytic ribozyme, Vif5113 reduced *vif* expression.

Transfection of 293T cells with a 1:1 mixture of the catalytic ribozyme, pSRP5113 and pCMV-VifFLAG indicated a reduction of *vif* activity (Figure 3, compare lanes 1 and 2). No such decrease in *vif* expression was observed when the ribozyme was transfected at a 2:1 ratio (pSRP5113 to pCMV-VifFLAG). In this instance the level of *vif* expression in cells transfected with the catalytic and non-catalytic ribozymes appeared to be the same. (Figure 3, compare lanes 3 and 4). This produced a confounding result, which has yet to be fully resolved.

### Discussion

HIV-1 *vif* encodes a protein that neutralizes an inhibitory host defense mechanism mediated by apolipoprotein B mRNA-editing enzyme-catalytic polypeptide-like 3G (APOBEC3G) (8). This protein is a cellular cytidine deaminase that is encapsulated into assembling virions in the absence of *vif* and is inhibitory during the next round of viral replication. *Vif* neutralizes APOBEC3G by reducing its translation and by rapid degradation of the native protein (10).

Because *Vif* inhibits APOBEC3G, its cleavage by hammerhead ribozymes may decrease the infectivity of HIV-1 virions. To test this hypothesis an anti-*Vif* ribozyme targeted to nucleotide 5113 within the HIV NL43 *vif* open reading frame and its non-catalytic control were cloned into the retroviral vector pSuper.retro.puro for tissue culture analysis. Our preliminary analysis suggested that the ribozyme was able to decrease *vif* expression in a transient assay. This was supported by a series of co-transfections using a 1:1 ratio of ribozyme and *vif* expression plasmids. However, a similar series of co-transfections using a 2:1 ratio of these plasmids produced conflicting results. In this second transfection series, the samples revealed bands of approximate equal intensity suggesting that the ribozyme had no effect on *vif* expression.

However, after further analysis it was determined that there were discrepancies in the total amount of protein added to lane 2 (1:1 pSRP5113Δ to pCMV-VifFLAG) and 3 (2:1

---

pSRP5113 to pCMV-VifFLAG). In both cases the amount of protein was determined to be approximately 50% less than originally calculated. Notwithstanding, when comparing the 1:1 catalytic transfection, the data suggest that the ribozyme may be inhibiting *vif* expression (Figure 3, compare lane 1 and 2). With more protein in the Vif5113 sample (lane 1) as compared to the Vif5113Δ samples (lane 2), the differences are even greater than at first appeared. This also holds true when comparing lane one (Vif5113) with the other sample transfected with the non-catalytic ribozyme (lane 4). Importantly, approximately equal amounts of protein were loaded in these two lanes (1 and 4). These data suggest that the ribozyme may be reducing *vif* expression in this cellular model. However; the relatively equal amounts of *vif* expression observed in lanes 3 and 4 do not support this conclusion. These two samples were obtained from cells that contained catalytic and non-catalytic ribozymes transfected at a 2:1 ratio. Therefore, further analyses are required to reproduce this data and ascertain the efficiency of ribozyme-mediated degradation of *vif* mRNA

## References

Funding for this project was obtained from the USCA Department of Biology and Geology and by a USC Magellan Research Scholarship.

1. Daigleish,A.G., Beverly,P.L.C., Clapham,P.R., Crawford,D.H., Greaves,M.F. and Weiss,R.A., *Nature*, 1984, **312**, 763.
2. Maddon,P.J., Daigleish,A.G., McDougal,J.S., Clapham,P.R., Weiss,R.A. and Axel,R., *Cell*, 1986, **47**, 333.
3. Barre-Sinoussi,F., Chermann,J.C., Rey,F., Nugeyre,M.T., Chamaret,S., Gruest,J., Dautet,C., Axler-Blin,C., Vizinnet-Brun,F., Rouzioux,C. *et al.*, *Science*, 1983, **220**, 868.
4. Popovic,M., Sarnadharan,E., Read,E. and Gallo,R.C., *Science*, 1984, **224**, 496-500.
5. Sarnadharan,E., Popovic,M., Bruch,L., Schupbach,J. and Gallo,R.C., *Science*, 1984, **224**, 506.
6. Levy,J.A., Hoffman,A.D., Kramer,S.M., Landis,J.A. and Shimabukuro,J.M., *Science*, 1984, **225**, 840.
7. UNAIDS/WHO. UNAIDS, Geneva 2007, UNAIDS/07.27E., ISBN 978 92 9 173621 8
8. Goncalves,J. and Santa-Marta,M., *Retrovirology*, 2004, **1**, 28.
9. Navarro,F. and Landau,N.R., *Curr. Opin. Immunol.*, 2004, **16**, 477.
10. Shirakawa,K., Takaori-Kondo,A., Kobayashi,M., Tomonaga,M., Izumi,T., Fukunaga,K., Sasada,A., Abudu,A., Miyauchi,Y., Akari,H. *et al.*, *Virology*, 2006, **344**, 263.
11. Jackson,W.H., Jr., Moscoso,H., Nechtman,J.F., Galileo,D.S., Garver,F.A. and Lanclos,K.D., *Biochem. Biophys. Res. Commun.*, 1998, **245**, 81.
12. Zhou,C., Bahner,I.C., Larson,G.P., Zaia,J.A., Rossi,J.J. and Kohn,E.B., *Gene*, 1994, **149**, 33.
13. Lo,K.M., Biasolo,M.A., Dehni,G., Palu,G. and Haseltine,W.A., *Virology*, 1992, **190**, 176.
14. Haseloff,J. and Gerlach,W.L., *Nature*, 1988, **334**, 585.
15. Perriman,R., Delves,A. and Gerlach,W.L., *Gene*, 1992, **113**, 157.
16. Swindle,C.S., Kim,H.G. and Klug,C.A., *J. Biol. Chem.*, 2004, **279**, 34.
17. Brummelkamp,T.R., Bernards,R. and Agami,R., *Science*, 2002, **296**, 550.
18. Anderson,K.L. and Jackson,W.H., *Journal of the South Carolina Academy of Science*, 2005, **3**, 24.
19. Berkner,K.L. and Sharp,P.A., *Nucleic Acids Res.*, **11**, 1983, 6003.
20. Hosfield,T. and Lu,Q., *Biotechniques.*, 1998, **25**, 306.
21. Sambrook,J., Fritsch,E.F. and Maniatis,T. (1989) *Molecular Cloning: A Laboratory Manual*. Cold Spring Harbor Press, New York.

---

# Generation of a retroviral vector that expresses an anti-HIV-1 *tat* hammerhead ribozyme

Padgett, Lindsey E.<sup>a</sup> and William H. Jackson<sup>\*b</sup>

<sup>a</sup> University of Alabama Birmingham, Birmingham, AL USA. E-mail: lpadgett@uab.edu

<sup>b</sup> Department of Biology and Geology, University of South Carolina Aiken, Aiken, SC, USA. Fax: 803-641-3251; Tel: 803-641-3601; E-mail: billj@usca.edu

Received September 1, 2009

Ribozymes have emerged as promising therapeutics for HIV and have been shown to bind and cleave target RNA's in a sequence-specific manner. The HIV-1 regulatory protein *tat* plays an essential role in the upregulation of viral transcription and elongation of viral transcripts, and has therefore been identified as a target for ribozyme studies. To further study the use of these reagents, we have designed a number of hammerhead ribozymes targeted to specific sequences within the HIV-1 NL43 *tat* sequence. One of these, Tat5910 and its non-catalytic control Tat5910Δ, were cloned into the retroviral vector pSuper.retro.neo+GFP (pSRNG) for cell culture studies. Recombinant retrovirus particles were generated by transient transfection of 293T cells using a two-plasmid system consisting of the helper plasmid, pPAM3, and pSRNG5910Δ. Identical experiments were carried out using two Mo-MLV retroviral vectors, pLNCE, and pLNCLZRz. The resulting recombinant virus was used to transduce NIH-3T3 cells, and virus titer (virus particles/ml) was determined from the number of Green Fluorescent Protein (GFP)- or β-galactosidase-positive cells. Although producer cells transfected with pSRNG5910Δ expressed GFP, the transfection efficiency was low. This resulted in levels of transduced NIH-3T3 cells that were too low to obtain a reliable titer measurement. Attempts to optimize titer by increasing the number of transfected producer 293T cells was successful using pLNCE and pLNCLZRz. Positive GFP or β-galactosidase expression in NIH-3T3 cells transduced with LNCE and LNCLZRz recombinant virus indicated that our two-plasmid virus production system was successful. Extremely low titer along with lower cellular expression of GFP suggests that the pSRNG5910 vectors may be better suited to virus production using a stable producer cell line such as PA317

## Introduction

Human Immunodeficiency Virus (HIV-1) infection results in the gradual loss of T<sub>H</sub> cells, decreased immune competence, and increased susceptibility to various opportunistic infections, including *Pneumocystis jirovecii* pneumonia, tuberculosis, and cytomegalovirus. Infection by these opportunistic infections, in addition to a T<sub>H</sub> lymphocyte count below 200/mm<sup>3</sup>, define the Acquired Immune Deficiency Syndrome (AIDS) (1).

Traditional HIV treatments have sought to reduce viral load by utilizing drugs that prohibit effective viral replication (2). For example, Triple Combination Therapy (TCT), which involves one protease inhibitor and two reverse transcriptase (RT) inhibitors, has been shown to effectively reduce viral load (2). Nevertheless, resistance to protease and RT inhibitors have already developed, requiring a continued search for therapies that can inhibit other HIV gene functions (3). For HIV, these functions are generally associated with the six accessory genes that control infection and replication: *tat*, *rev*, *nef*, *vif*, *vpr*, and *vpu* (4).

Tat increases viral transcription from the HIV-1 Long Terminal Repeat (LTR) by binding to the *cis* acting RNA enhancer element, the transactivation response region (TAR), which is transcribed from the R (Repeat) region of the 5' LTR (5). Once transcribed, TAR forms a hairpin loop consisting of a base-paired stem, a three nucleotide non-base-paired bulge, and a six-nucleotide Guanine-rich loop (2) that is present at the 5' end of all viral transcripts. The Tat/TAR interaction recruits numerous cellular transcriptional coactivators to TAR, including P-TEFb (Positive Transcription Elongation Factor b), an RNA

polymerase II C-terminal kinase, resulting in the phosphorylation of the C-Terminal Domain (CTD) of RNA Polymerase II (6). The phosphorylation of the CTD increases RNA polymerase II processivity, thereby inducing elongation of viral transcripts (7). Tat is absolutely required for HIV replication and is, therefore, an important target for novel anti-HIV reagents.

Targeting HIV-1 at the genomic level can be accomplished by hammerhead ribozymes, which are small catalytic RNAs that can be targeted to cleave viral mRNAs (8). These RNA enzymes target and cleave mRNA at any XUX', where X is any nucleotide, and X' is Adenine, Cytosine, or Uracil (8). Hammerhead ribozyme design, based on the Hasseloff and Gerlach model (9), consists of two flanking regions that provide target specificity by Watson-Crick base pairing and a catalytic core that cleaves at the target site. Cleavage of *tat* mRNA sequences by hammerhead ribozymes may negatively impact transcription initiation and elongation, leading to the inability of HIV to replicate within cells (10;11).

Previously, our lab designed and cloned a number of hammerhead ribozymes targeted to the *tat* genomic sequence of the HIV-1 genomic clone NL43. Each of these ribozymes and a corresponding non-catalytic control ribozyme was cloned into the shuttle vector, pPCR-Script. For initial cell culture testing, Tat5910 and its non-catalytic control Tat5910Δ, were subcloned into the retroviral vector pSuper.Retro.Neo+GFP (pSRNG). This modified Moloney Murine Leukemia virus (Mo-MLV) vector can infect non-dividing cells (e.g., hematopoietic stem cells) and is self-inactivating due to a deletion in the 3' LTR (12). Importantly this vector has been designed to express siRNAs from the RNA Polymerase III H1 promoter (13), making it a logical choice for expressing other small RNAs such as hammerhead ribozymes. For selection purposes pSRNG expresses neomycin

phosphotransferase and green fluorescent protein (GFP) from a single IRES-containing transcript controlled by the phosphoglycerokinase (PGK) promoter (13).

This paper describes cloning of an anti-HIV hammerhead ribozyme Tat5910 into the retroviral vector, pSuper.retro.neo+GFP, along with initial cell culture testing. These tests involved analysis of transgene expression and optimizing virus titer produced in a transient producer cell system. For this we utilized a two-plasmid system consisting of a retroviral vector and a helper plasmid (14).

#### Tat substrate RNA

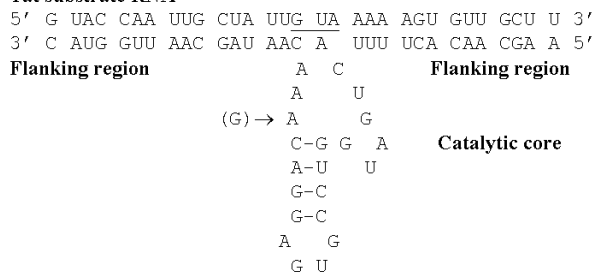


Figure 1. Hammerhead ribozyme design. Tat RNA showing the pGUA cleavage site at nucleotide 5910 is shown annealed to the ribozyme flanking regions. The catalytic core was made inactive by an A to G mutation (11).

## Materials and Methods

### Oligonucleotides and cloning

A hammerhead ribozyme, based on the Haseloff and Gerlach model (9) was designed to cleave a pGUA sequence at nucleotide 5910 within the HIV genomic clone NL43 (Accession number M19921) (Figure 1). The Tat5910 sense (5'-gat ccA AGC AAC ACT TTT CTG ATG AGT CCG TGA GGA CGA AAC AAT AGC AAT TGG TAC Aa- 3') and antisense sequences (5'-agc ttT GTA CCA ATT GCT ATT GTT TCG TCC TCA CGG ACT CAT CAG AAA AGT GTT GCT Tg- 3') were synthesized with BamHI and HindIII sites to facilitate cloning. Two-hundred picomoles of each oligonucleotide were combined in annealing buffer (100mM NaCl, 50mM HEPES buffer (pH 7.4)) and cooled slowly from 90 to 4°C. The annealed oligonucleotides were ligated into the BglIII and HindIII sites of the retroviral vector pSuper.retro.neo+GFP (pSRNG) according to the manufacturer's protocol (Oligoengine). A non-catalytic ribozyme targeted to the same sequence was created by an A to G mutation in the catalytic core. This oligonucleotide was synthesized and similarly cloned into pSRNG.

Ligation was carried out using T4 DNA Ligase (Promega) in a 4°C overnight reaction. The ligated plasmids were transformed into JM109 cells and the resulting colonies were screened for the presence of the ribozyme. For this, miniprep DNA was screened by PCR using a plasmid-specific primer pair that framed the cloning site. The PCR reaction consisted of 100 pMol of each primer and 2X PCR Master Mix (50units/mL Taq DNA Polymerase) (Promega). Positive clones were indicated by the presence of a 482 bp fragment. Correct ribozyme insertion into the resulting plasmids, pSRNG5910 and pSRNG5910Δ, was verified by sequencing.

### Cell lines and transfections

293T and NIH-3T3 cells were maintained in Dulbecco's Modified Eagle Medium (DMEM) supplemented with 10% Fetal Bovine Serum (FBS) in a humidified 37°C incubator with 5% CO<sub>2</sub>. All transfections were done by calcium phosphate precipitation based on the method of Berkner and Sharp (15). Briefly, 293T cells were plated to 50-70% confluency onto 60 mm dishes 24 hours prior to transfection. The cells were transiently transfected with 4 μg of plasmid DNA in 125 mM CaCl<sub>2</sub>, and 2X HBS (280 mM NaCl/ 1.5 mM Na<sub>2</sub>HPO<sub>4</sub>/ 50 mM HEPES Buffer (pH 7.05)). The resulting precipitate was added to the culture medium and allowed to be taken up by the cells. Transfection efficiency, as measured by GFP (pLNCE and pSRNG5910) or β-galactosidase (pLNCLZRz) expression was analyzed as a function of transfection time. For this, 293T cells were allowed to remain in contact with the DNA precipitate for 4, 8, 12, or 24 hours. Transgene expression was assayed 24 hours after removal of the DNA precipitate.

GFP expression was analyzed directly using an Olympus CKX41 inverted microscope with epifluorescence. β-galactosidase expression was measured by the ability to metabolize X-gal (10) For this, cells were washed twice with PBS and fixed for 15 minutes with 0.1 M Sodium Phosphate, pH 7.0/1 mM MgCl<sub>2</sub>/0.25% glutaraldehyde. Subsequently, the cells were washed three times with PBS, and stained by the addition of X-gal (PBS/4 mM K<sub>4</sub>Fe(CN)<sub>6</sub>·3H<sub>2</sub>O/4 mM K<sub>3</sub>Fe(CN)<sub>6</sub>/10 mM MgCl<sub>2</sub> /0.03% X-gal). The presence of blue-stained cells after 24 hours indicated positive transfection.

### Recombinant Virus Production

Recombinant viruses were produced in 293T cells using a transient two-plasmid system consisting of a retroviral vector and a helper plasmid (10;14). Three retroviruses were analyzed for their ability to generate retroviruses in this system: pSRNG5910Δ, pLNCE, and pLNCLZRz. All are Mo-MLV viruses that express either GFP (pSRNG5910Δ, pLNCE) or β-galactosidase (pLNCLZRz). pPAM3 is a Mo-MLV based helper plasmid that expresses all retroviral structural genes, including an amphotropic glycoprotein (16).

To generate recombinant retrovirus particles for transduction into target cells, 0.5 x 10<sup>6</sup> 293T cells were plated onto 60mm dishes. After 24 hours, these cells were transfected as described using 4 μg helper plasmid (pPAM3) and 4 μg retroviral vector (pSRNG5910Δ, pLNCE, or pLNCLZRz). The resulting precipitate was allowed to be taken up by the cells from 4 to 24 hours, after which time the medium was replaced. Twenty-four hours later, the virus-containing medium was harvested from the producer cells, filtered through a 0.45 μm syringe filter, and stored at -80°C.

The presence of virus particles in the harvested medium was determined following transduction of target cells. For this, 0.25 x 10<sup>6</sup> NIH-3T3 cells were plated onto 35mm dishes. After 24 hours, these cells were transduced by the addition of one milliliter each of harvested medium and fresh culture medium containing 8 μg polybrene (4 μg/ml). The cells and virus particles were incubated together for 24 hours, after which the medium was replaced. After an additional 24 hours, virus titer was

determined from the number of GFP or X-gal positive cells. Virus titer was determined from the average number of positive target cells in 10-20 randomly chosen fields at 200X using bright-field or epifluorescence microscopy. This number was extrapolated to determine the total number of positive cells.

### Optimizing virus titer

Transfection incubation time, referring to the length of time the transfection reagent remained on producer cells, was altered to optimize virus titer. 293T cells were incubated with DNA precipitate at four different time points: 4, 8, 12, and 24 hours. After each time point, the medium was replaced and the cells incubated for an additional 24 hours. The virus containing medium was harvested and used to transduce NIH-3T3 cells as described. GFP or  $\beta$ -galactosidase expression was monitored, and virus titer was determined.

## Results

The HIV-1 NL43 genomic sequence was analyzed for the presence of potential hammerhead ribozyme target sites. One site, a pGUA located at nucleotide 5910 was used to design an anti-tat hammerhead ribozyme. This ribozyme and its non-catalytic control (Figure 1) were synthesized and cloned into the retroviral vector, pSuper.retro.neo+GFP. Sequencing was used to verify the ribozyme sequence in each of the resulting plasmids: pSRNG5910 and pSRNG5910 $\Delta$  (Figure 2). Once cloned,

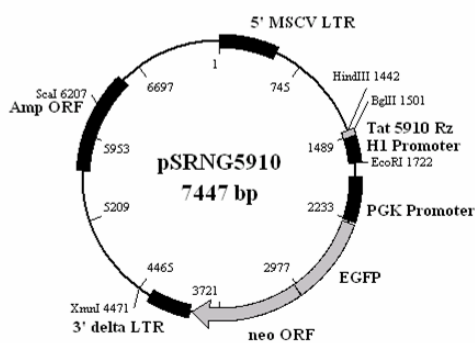


Figure 2. Retroviral vector pSRNG5910. Tat5910 oligonucleotides were synthesized and cloned into the BglII and HindIII sites of pSuper.retro.neo+GFP. The resulting vector is shown. A similar vector, pSRND5910 $\Delta$ , was created by cloning the non-catalytic version of the ribozyme.

pSRNG5910 $\Delta$  was tested to ensure GFP expression was not affected by the cloning process. 293T cells were transiently transfected using the calcium phosphate method and after 48 hours analyzed for transgene expression. These results indicated relatively high levels of GFP expression (Figure 3). However, GFP levels were noticeably lower than in cells transfected in parallel with pLNCE (data not shown).

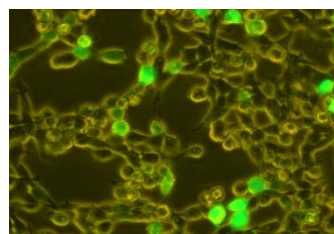


Figure 3. GFP expression. 293T cells were transfected with pSRNG5910 $\Delta$  by calcium phosphate precipitation. GFP expression was monitored 48 hours later.

The ability to generate recombinant retroviral particles in a transient transfection system was next investigated using a retroviral vector (pSRNG5910 $\Delta$ , pLNCE, or pLNCLZRz) and a helper plasmid (pPAM3) to produce viral particles in 293T cells. Forty-eight hours after transfection, the virus-containing medium was harvested and used to transduce NIH-3T3 cells. The producer and target cells were analyzed for either GFP or  $\beta$ -galactosidase expression (Figure 4) as a measure of transfection (293T cells) or transduction (NIH-3T3 cells). In these tests, virus production was observed using both pLNCE and pLNCLZRz. However virus production using the pSRNG5910 $\Delta$  vector was not observed in this series of experiments (Figure 4).

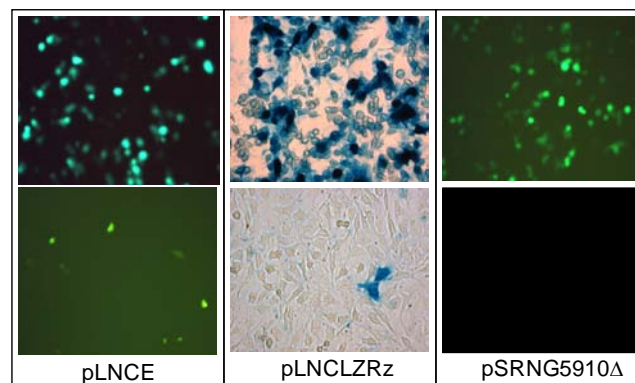


Figure 4. Production of recombinant retrovirus. 293T cells were transiently transfected with pPAM3 and one of three retroviral vectors. Transfection efficiency was determined by the relative number of GFP- or X-gal positive cells (Upper panels). Virus containing medium was harvested and used to transduce NIH-3T3 cells. Virus-mediated expression was only evident in pLNCE and pLNCLZRz transduced cells (Lower panels). GFP-positive cells are green. X-gal positive cells are blue.

To optimize virus titer, the length of transfection incubation period, as measured by the time the DNA precipitate was incubated with the 293T cells, was altered. For this, the transfection reagent was left on the 293T cells for 4, 8, 12, or 24 hours. The precipitate was removed by a change of medium and 24 hours later, virus was harvested in the culture medium. At this time the 293T producer cells were analyzed for GFP or  $\beta$ -galactosidase expression to make sure the transfection was successful. Regardless of the transfection incubation period, all 293T transfection experiments yielded positive GFP or  $\beta$ -galactosidase expression. For the retroviral vector pSRNG5910 $\Delta$ , higher GFP expression was observed in the 12 hour incubation period compared to the four and eight hour periods. However, no visible differences were evident in GFP expression among the 12 and 24 hour incubation periods (data not shown).

The ultimate purpose of these transfection studies was to determine if virus production was increased by allowing the 293T producer cells to remain in contact with the transfection reagents for longer periods of time. To determine the virus titer produced in these experiments, NIH-3T3 cells were incubated with virus-containing medium harvested from the producer cells. With regards to virus production, extremely low levels of GFP expression was observed in the NIH-3T3 cells transduced with the harvested medium from producer cells transfected with pPAM3 and pSRNG5910Δ. This was true of all incubation periods, and resulted in an inability to determine a reliable titer for this vector (Figure 4). On the other hand, with the exception of the eight hour incubation period, recombinant virus was produced in target cells transduced with pLNCE or pLNCLZRz, as measured by the number of GFP or X-gal positive cells (Figure 5). Analysis of virus titer generated by pLNCLZRz transfections for all incubation periods indicated an increase over time. The maximum titer obtained with this vector was measured at the 24 hour time point as  $1 \times 10^4$  virus particles per milliliter (Figure 5). The virus titer produced using pLNCE indicated a large increase at the 12 hour time point; however, the titer at the 24 hour time point was approximately 50% less (Figure 5). At all time points tested, the pSRNG5910Δ vector failed to produce a measurable titer.

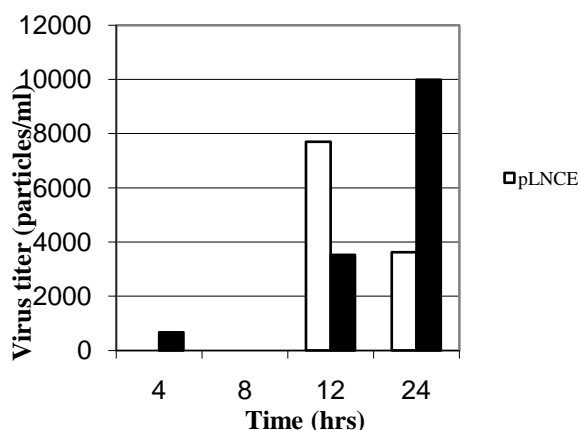


Figure 5. Optimization of virus titer. The number of virus particles per milliliter of harvested culture medium was determined for pLNCE and pLNCLZRz transduced NIH-3T3 cells. Virus titer was optimized by increasing the transfection incubation time from 4 to 24 hours. Virus titer was found to be directly related to this increase.

## Conclusions

Previous studies have shown that hammerhead ribozymes targeted to HIV-1 accessory genes such as *tat* can down regulate virus replication. Many of these studies have used retroviral vectors to express ribozymes as part of an RNA Polymerase II transcript (10;11). While effective, these transcripts are often large and likely produce secondary structures that may interfere with efficient ribozyme cleavage. The pSUPER family of vectors were specifically created to express siRNAs from the RNA Polymerase I H1 promoter and should represent a good choice to express hammerhead ribozymes. Additionally, the

pSUPER retroviral vectors are self-inactivating and express neomycin phosphotransferase and GFP from the PGK promoter.

The primary goal of this project was to clone a hammerhead ribozyme targeted to HIV-1 *tat* into pSRNG and to characterize the resulting vector prior to its use in anti-HIV experiments. A second goal was to determine the optimal conditions to produce recombinant retrovirus particles in a transient two-plasmid system. The resulting plasmids, pSRNG5910 and pSRNG5910Δ were generated for this purpose. Initial tests indicated that both retroviral vectors expressed GFP when transiently transfected into 293T cells. However, in all cases the non-pSUPER retrovirus, pLNCE, generated greater GFP expression than either pSRNG5910 or pSRNG5910Δ in transfected 293T cells. Although it does not explain the overall lower transfection efficiency of pSRNG5910Δ, it is likely that pLNCE generated greater levels of GFP expression due to transcriptional control of the immediate early CMV promoter. In comparison, GFP expression in the pSUPER vector is controlled by the comparatively weaker PGK promoter. In fact, a number of cells transfected with pSRNG5910Δ appeared to be very weakly positive for GFP expression, although they were not counted as GFP-positive for these studies. The other retroviral vector used in these experiments, pLNCLZRz also yielded higher numbers of transfected cells, and like pLNCE, this plasmid possesses a CMV promoter that controls expression of β-galactosidase.

The use of these plasmids as retroviral vectors was next studied by comparing the ability of pSRNG5910Δ to produce virus with the retroviral vectors pLNCE and pLNCLZRz. In these studies, pSRNG5910Δ failed to produce measurable virus. Although a very small number of GFP-positive target cells were identified, the number was too small to determine a reliable titer. Subsequently, the length of transfection incubation period was altered in an attempt to optimize virus titer. Transfection with the helper plasmid, pPAM3, and either pLNCE or pLNCLZRz produced measurable virus titers, up to a high of  $10^4$  particles per milliliter. Again, pSRNG5910Δ failed to produce measurable virus titers in these experiments. Overall; however, these results did indicate that our two-plasmid system successfully generated recombinant virus.

It is quite possible that the two different ways virus expression was measured and used to determine titer played a role in the discrepancies seen in the virus titer optimization experiments (Figure 5). Target cells transduced with recombinant virus produced using the pLNCLZRz vector resulted in the ability to metabolize X-gal.; therefore staining produced blue cells that were easy to identify and count using brightfield microscopy. There is a higher degree of uncertainty involved in scoring GFP-positive cells produced from transduction with recombinant virus from pLNCE and pSRNG5910Δ. It may be that when using these vectors, a more reliable way of determining titer would be to generate neomycin resistant colonies.

Ultimately, because pSRNG5910Δ failed to generate measurable levels of recombinant virus, optimization studies will be impractical until a method for producing virus with this vector can be developed. Although transient systems may be successfully used to generate virus using pSRNG-based vectors, future studies will need to increase transfection efficiency. One such method may be through the use of lipid-based transfection

---

procedures. Alternatively, it may be necessary to generate a stable producer line for efficient virus production.

## References

1. CDC , *Morbidity and Mortality Weekly Report* 1992, **41**, RR- 17.
2. Freed,E.O., *Somat. Cell Mol. Genet.*,2001, **26**, 13.
3. Rigden,J.E., Ely,J.A., Macpherson,J.L., Gerlach,W.L., Sun,L.Q. and Symonds,G.P., *Curr. Issues Mol. Biol.*,2000, **2**, 61.
4. Trono,D., *Cell*,1995, **82**, 189.
5. Fraiser,C., Irvine,A., Wrighton,C., Craig,R. and Dzierzak,E., *Gene Ther.*,1998, **5**, 1665.
6. Herrmann,C.H. and Rice,A., *J. Virol.*,1995, **69**, 1612.
7. Frankel,A.D. and Young,J.A., *Annu. Rev. Biochem.*, 1998, **67**, 1.
8. Perriman,R., Delves,A. and Gerlach,W.L., *Gene*, 1992, **113**, 157.
9. Haseloff,J. and Gerlach,W.L., *Nature*,1988, **334**, 585.
10. Jackson,W.H., Jr., Moscoso,H., Nechtman,J.F., Galileo,D.S., Garver,F.A. and Lanclos,K.D., *Biochem. Biophys. Res. Commun.*, 1998, **245**, 81.
11. Zhou,C., Bahner,I.C., Larson,G.P., Zaia,J.A., Rossi,J.J. and Kohn,E.B., *Gene*, 1994, **149**, 33.
12. Swindle,C.S., Kim,H.G. and Klug,C.A., *J. Biol. Chem.*, 2004, **279**, 34-41.
13. Brummelkamp,T.R., Bernards,R. and Agami,R., *Science*, 2002, **296**, 550.
14. Pear,W.S., Nolan,G.P., Scott,M.L. and Baltimore,D., *Proc. Natl. Acad. Sci. U. S. A.*, 1992, **90**, 8392.
15. Berkner,K.L. and Sharp,P.A., *Nucleic Acids Res*, 1983, **11**, 6003.
16. Miller,A.D. and Rosman,G.J., *Biotechniques.*, 1989, **7**, 980.

# The Effects of Growing Method and the Food Processing System on Bacterial Concentration in Spinach

Thad S. Moore\* and Lisa W. Norman

Heathwood Hall Episcopal School, 3000 S. Beltline Blvd., Columbia, SC.

Received June 6, 2009

The purpose of this study was to examine the bacterial effects of the industrial food processing system on bacterial contamination and the differences between conventionally and organically grown produce therein. This is significant because every day millions of people consume these products. The hypothesis was that organically grown and locally grown spinach will have the lowest levels of bacterial concentration, respectively, when compared to conventional and bagged spinach. Three samples each of local organic, loose, domestic organic, bagged organic and bagged conventional spinach were taken by rinsing a portion of each leaf in water. 500  $\mu$ L of this rinse was spread on nutrient agar plate and was incubated for 24 hours at 36°C. Bacterial colonies in 10 randomly selected 1 cm<sup>2</sup> areas were counted, and the colonies' morphologies were noted, as was any fungal growth. The data were averaged and analyzed using a one-way ANOVA test ( $\alpha=0.05$ ). There was no statistically significant difference between the bagged organic and conventional test groups. Local organic spinach had the least number of bacterial colonies with a total of 247 colonies, and bagged conventional had the most with 1813. These results support the hypothesis. Future research could test other types of produce as well. Other possibilities include focusing exclusively on testing organic produce against conventionally grown produce.

## Introduction

Every day, millions of people all around the world consume produce that has been processed, packaged and shipped. A study by the Freedomia Group found that packaged produce will be purchased by more consumers, as its market share in the United States will increase by 4.2% annually until 2012 (2). Packaged foods are already a staple of diets everywhere, and they are here to stay. Such growth in the industry comes even in the midst of far-reaching outbreaks related to such foods. In September and October 2006, 199 people from 26 states were infected by *Escherichia coli* 0157:H7 (*E. coli*) in an outbreak traced to fresh spinach. 3 died, including 1 child (3). In September 2008, Gadi Frankel, a professor at London's Imperial College, said that "people are eating more salad products, choosing to buy organic brands and preferring the ease of 'pre-washed' bagged salads from supermarkets. All of these factors, together with the globalisation of the food market, mean that cases of salmonella and E coli poisoning caused by salads are likely to rise in the future" (5). A study published in the Journal Applied and Environmental Microbiology links the age of lettuce leaves to the size of populations of *E. coli*. The study found that leaves on the inner part of the head consistently had 10 times more growth than older leaves on the middle part (6). As agriculture is increasingly commercialized and industrialized, leaves are picked earlier and earlier, and the likelihood of *E. coli* contamination increases drastically.

Produce is defined as any fruit or vegetable that is purchased fresh in either loose or packaged. Food processing is defined here as the system of industrially harvesting, packaging and shipping produce. This study will also examine organically and conventionally grown produce. Foods grown without chemical fertilizers and pesticides or certified organic by the US Department of Agriculture are organic. Foods grown with these chemicals are conventionally grown. Locally grown produce is defined as produce grown within

South Carolina. Domestically grown produce is defined as produce grown within the United States but outside of South Carolina.

Contamination is common in all aspects of food processing. A study by Lillard, "The Impact of Commercial Processing Procedures of the Bacterial Contamination and Cross-contamination of Broiler Carcasses," measured bacterial levels at six points in a broiler processing plant and found that bacterial concentration increased as carcasses moved through the plant (7). If processing has such dramatic effects on meat, what effects does processing have on produce? A study by Brackett, "Microbiological Consequences of Minimally Processed Fruits and Vegetables," partially answered this question when it found that minor changes in fruits' and vegetables' environments, such as temperature and humidity, can affect how prevalent microbes are (1). Though Brackett's research answered this question partially, no study has completely answered it. This study, however, will attempt to use the following methods: Loose organic, packaged organic and packaged conventional spinach were purchased from grocery stores in the Columbia, SC area. Leaves with excessive brownness and/or stagnant water were avoided. Local organic spinach was picked at a local community garden that uses organic growing methods. Three leaves from each of the 4 groups, along with 3 control tests, were tested. Bacterial levels and colony morphologies were compared between groups. Data were analyzed with a one-way ANOVA ( $\alpha=0.05$ ) test.

This research was conducted because food is a crucially important aspect of all people's lives. Millions of people around the world consume organic produce, packaged produce and domestically grown produce. As food is produced farther and farther away from people and people are more and more disconnected from their food source, it's important that they know what they are consuming, bacteria and all. The purpose of this research was to study bacterial levels in organically and conventionally grown produce and local, domestic and packaged produce.

It was hypothesized that organically grown and locally grown produce will have the lowest levels of bacterial concentration, respectively. The null hypothesis is that bacterial concentration will not vary between growing methods and growing locations. The independent variable is the growing method and the growing location. The dependent variable is the number of bacterial colonies that are present after incubation.

## Methods

Spinach leaves and bags were selected using guidelines suggested by experts in food safety and in the industry: leaves with excessive brownness were avoided, as were bags with excessive water in them. Once purchased, leaves were refrigerated until needed. The amount of time between purchase and testing was minimized. Before testing began, Petri dishes were poured with nutrient agar using instructions outlined in "Instructions for Bottled Media," a booklet written by Carolina Biological Supply. Poured plates were stored in a refrigerator until needed. Throughout preparation and testing, proper sterile technique was followed. 5 milliliters of sterile water was added to each sterile 50mL centrifuge tube. A 2x2cm square was then cut from each of the 12 spinach leaves [3 leaves per group (local organic, loose organic, bagged organic and bagged conventional)] and added to its corresponding tube. After the leaf was added, each tube was shaken for 10 seconds. The leaf was removed with sterilized forceps. 500 microliters of each sample was taken with the micropipette, added to a Petri dish containing nutrient agar and spread evenly on the plate. The plate was then taped and placed into an incubator set at 36°C and incubated for 24 hours. Each plate held only the sample from one leaf. After incubation, plates were stored in a refrigerator until they were ready to be counted. PetriStickers were placed on the bottom of each plate. A set of 10 random numbers was generated. These numbers represented 10 1 cm<sup>2</sup> squares on the sticker. These squares were counted by hand with the assistance of a stereo microscope. Colonies' morphology and any fungal growth were noted in addition to the bacterial counts. The same set of random numbers was used when counting the remaining plates. This process was repeated for each of the remaining 14 trials. This process was repeated thrice more without leaves to act as a negative control. The bacterial counts for each of the three plates within each group were averaged, and the standard deviation was calculated. The results were then analyzed using a one-way ANOVA ( $\alpha=0.05$ ) test.

## Results

Table 1 displays the total number of bacteria counted in a 10 cm<sup>2</sup> per plate, the total number of colonies counted by experimental group and the mean for each group, as well as counts and the mean for the control group. Asterisks (\*) denote plates that had observed fungal growth. As demonstrated by the data, bagged conventional leaves had the most bacterial growth (1813 colonies), followed, in order, by

bagged organic (953), loose organic (514) and, finally, local organic (247). All local organic plates had fungal growth, as did one bagged conventional plate. Standard deviation was highest in bagged conventional tests ( $\pm 212.74$ ), followed closely by bagged organic ( $\pm 211.33$ ). Loose organic plates had the third highest standard deviation ( $\pm 123.62$ ), and local organic had the lowest deviation of the experimental groups ( $\pm 10.02$ ). The control plates had the lowest deviation of all groups ( $\pm 3.61$ ).

Plate #	Loose Organic	Bagged Organic	Local Organic	Bagged Conventional	Control
1	306	296	*92	783	0
2	63	118	*72	*369	2
3	145	539	*83	661	7
TOTAL	514	953	247	1813	9
MEAN	171.3	317.7	82.3	604.3	3.0
STDEV	123.62	211.33	10.02	212.74	3.61

Table 2 displays the average number per plate of bacteria for each colony morphology observed, ordered by group. There were four colony morphologies observed in this study. The smooth white morphology was the most prevalent of the four observed. Smooth yellow was the second most common in three groups, while it was not present in local organic tests. Clear and fried egg morphologies followed in third and fourth, respectively. In each of the experimental groups, smooth white bacteria were the most common. In the control group, clear was the dominant morphology. The smooth yellow and fried egg morphologies were found most often in loose organic tests. Bagged conventional followed loose organic closely in its smooth yellow counts. Clear bacteria were most commonly found in bagged organic tests, as compared to the other groups.

A single factor ANOVA test ( $\alpha=0.05$ ) was used to

Bacteria Type	Loose Organic	Bagged Organic	Local Organic	Bagged Conventional	Control
Smooth White	110	349	81	547	0
Smooth Yellow	57	39	0	55	0
Fried Egg	4	3	0	1	0
Clear	0	19	1	1	3

analyze data and compare groups. 2 of the 4 experimental groups, loose organic and bagged organic, were found to have a statistically insignificant difference from the control group ( $p>0.05$ ). Bagged conventional and local organic data, however, did yield statistically significant results when compared to the control group, with p-values of .008 and .0001, respectively. When bagged conventional and bagged organic data were compared, there was no statistically significant difference at  $\alpha=0.05$ , suggesting that the difference in bacterial levels of organically and conventionally grown

P-values	Loc Org	Loose Org	Bagged Org	Bagged Con	Control
Loc Org		0.282	0.126	0.013	0
Loose Org			0.359	0.038	0.078
Bagged Org				0.173	0.061
Bagged Con					0.008
Control					

spinach is insignificant. No tests comparing any two organic groups (local, loose and bagged) yielded statistically significant results. A test between the loose organic and bagged conventional groups yielded a p-value of .038, suggesting a statistically significant difference. Local organic spinach showed similar results, yielding a p-value of .013 when compared to bagged conventional spinach.

## Conclusions

The purpose of this research was to examine the bacterial repercussions of the industrialization that dominates the food system today, as well as to examine the difference of organically and conventionally grown foods. The difference in bacterial levels of organically and conventionally grown spinach was insignificant. No tests comparing any two organic groups (local, loose and bagged) yielded statistically significant results. The data would suggest that spinach purchased locally or loose and domestically that were grown organically have a statistically significant lower amount of bacteria than bagged conventional. That no two similar (organic or bagged) groups had statistically significant differences suggests that bacterial concentration increased in small increments. Nonetheless, when extremes (loose organic and local organic v. bagged conventional) were compared, differences were statistically significant. These data would tend to support the hypothesis that organically grown and locally grown produce will have the lowest levels of bacterial concentration, respectively.

Attempts were made to decrease sources of error, but possible sources of error existed nonetheless. Before testing, leaves were not rinsed, so local organic leaves, which were picked at Heathwood's community garden, had soil visibly present, which is likely the source of the observed fungal growth. Another possible source of error was the type of spinach tested. Both the loose and bagged organic test groups used baby spinach, as opposed to the bagged conventional group, which was marketed simply as spinach. Another possible source is that there simply were not enough tests for definite conclusions to be made.

Future research possibilities abound. One possibility is to test other types of produce to determine if similar results are found. Another is to test for pathogenic bacteria, such as *E. Coli* or *Salmonella*. Such testing would take into account 'good bacteria.' Future research could also examine the effects that chemical pesticides and fertilizers have on bacterial concentration. Moving forward, food processing practices

should be reviewed to explain why and where bacterial contamination is occurring. No matter the source of contamination, these data display some of the adverse reciprocal effects of being separated from food sources. If this study causes one consumer to reconsider what he or she purchases and eats, whether that means they start to buy locally or organically, start their own garden, or otherwise alter their habits, or simply to wash his or her produce, it will be considered a success. Food is an essential component of all people's lives, and the more knowledgeable they are about what they eat, the better off they are.

## Acknowledgements

I would like to thank Mr. Jim Morris for use of his lab and Heathwood Hall Episcopal School for funding and use of its community garden. I would also like to thank Mrs. Michelle Myer for her incredibly useful advice. Finally, I simply cannot thank my Biology teacher, Mrs. Lisa Norman, enough for her patience, advice and wisdom, all of which were invaluable during the course of planning, experimentation and analysis.

## References

1. Brackett, R.E. "Microbiological Consequences of Minimally Processed Fruits and Vegetables." Journal of Food Quality (1987):195-206
2. "CDC | E. coli Outbreak From Spinach - Update: Oct. 6, 2006 | CDC Foodborne and Diarrheal Diseases Branch." Centers for Disease Control and Prevention. 05 Feb. 2009 <<http://www.cdc.gov/ecoli/2006/september/updates/100606.htm>>.
3. "Produce Packaging to 2012 - Market Research, Market Share, Market Size, Sales, Demand Forecast, Market Leaders, Company Profiles, Industry Trends and Companies including Weyerhaeuser, Smurfit-Stone and International Paper." The Freedonia Group - Market Research. 05 Feb. 2009 <<http://www.freedoniagroup.com/produce-packaging.html>>.
4. Imperial College London. 05 Feb. 2009 <[http://www3.imperial.ac.uk/newsandeventspggrp/imperialcollege/newssummary/news\\_3-9-2008-10-4-59?newsid=43294](http://www3.imperial.ac.uk/newsandeventspggrp/imperialcollege/newssummary/news_3-9-2008-10-4-59?newsid=43294)>.
5. Knudson, William A. The Organic Food Market. Apr. 2007. Michigan State University. 5 Feb. 2009.
6. "Leaf Age May Contribute To Contamination Of Lettuce With E. Coli And Salmonella." Science Daily: News & Articles in Science, Health, Environment & Technology. 05 Feb. 2009 <<http://www.sciencedaily.com/releases/2008/04/080425103338.htm>>
7. Lillard, H.S. "The Effects of Commercial Processing Procedures on the Bacterial Contamination and Cross-contamination of Broiler Carcasses." Journal of Food Protection (1990): 202-207.

---

# Temperature Changes Resulting from a GaAlAs Laser in the Decontamination of a Failing Dental Implant

Oppenheimer, Adam B.

Hilton Head Preparatory School, Hilton Head Island, SC

Received August 18, 2009

A periodontal implant can become infected by oral bacteria and the surrounding bone will dissolve, resulting in a failed implant. In contemporary practices, the only therapy is to scrape the infected site with a scaler- a very primitive method of debridement. The purpose of this experiment was to determine if the technique of lethal photosensitization is practical for the treatment of a failing dental implant. Previous studies have demonstrated that  $47\frac{1}{2}^{\circ}\text{C}$  is the threshold temperature for healthy bone cells. Exceeding this temperature results in cell death and the eventual loss of implant integration. It was predicted that that the  $47\frac{1}{2}^{\circ}\text{C}$  temperature threshold would be exceeded after prolonged exposure to laser energy. This was so because charring and odors were observed as a result of the lasing of a dental implant in a previous study. In this experiment, a Ti-plasma sprayed dental implant was inserted into a bone block cut from a pig femur. An artificial periimplant bone defect was cut into the bone to simulate a failing dental implant and to provide access for the laser treatment. A 940nm GaAlAs laser was used at wattages of .2, .5, 1.0, 1.5 and 2.0 in both continuous and pulsed mode. The bone block was placed in a water bath maintained at  $37\frac{1}{2}^{\circ}\text{C}$  the human body's thermal conductivity. A J/K-type thermocouple was inserted in the bone adjacent to the implant and connected to a digital meter to register temperature changes at the surface of the implant every 15 seconds for 180 seconds. The results indicate that when the laser was used in continuous mode, the threshold temperature of  $47\frac{1}{2}^{\circ}\text{C}$  was exceeded at wattages of 1.0, 1.5 and 2.0 watts. In pulsed mode, only the wattage to exceed the critical temperature was 2.0 watts. This was true regardless of the time of laser exposure. The hypothesis was rejected. Although some of the wattages did exceed the threshold temperature, the use of lower wattages and the use of a pulsed beam reduced the maximum temperature to below  $47\frac{1}{2}^{\circ}\text{C}$ . After comparing the data to the data of similar experiments performed with different types of lasers, it can be concluded that a pulsed setting will allow for optimum wattage output and maximum bacterial death without exceeding the critical temperature needed to maintain implant integration.

## Introduction and Related Research

Lasers, an acronym for Light Amplification by the Stimulated Emission of Radiation, have an extensive history that is still being developed today. The first conception of the laser was by Newton in 1704, when he stated that laser light was not like ordinary light. He said that it was an organized beam of particles. The earliest operating laser was created by Theodore Maiman on May 16, 1960 at the Hughes Research Laboratory in California. The next revolution was semi-conductor lasers, first designed by Robert Hall and his associates at the General Electric laboratories in Schenectady, New York in 1962. "Diode lasers now involve many different materials and forms, can be quite small and inexpensive, and are by far the most common type of laser. They are used, for example, in supermarket bar-code readers, in optical-fiber communications, and in laser pointers." [1].

Oral bacteria that are responsible for dental caries and periodontal disease (including the breakdown of bone around dental implants) may be photo-sensitive; they may die when exposed to diode laser light. Others have studied the effect of a similar laser on the regeneration of bone around failing dental implants. They used an 830 nm laser and tested in live dogs. The results were clear; the bone regeneration rate was 41% higher with laser treatment. "The lethal photosensitization associated with GBR allowed for better re-osseointegration at the area adjacent to the peri-implant defect regardless of the implant surface." [2]

Of greatest interest, is the experiment completed last year by Adam Oppenheimer. Oral bacteria were cultured and applied to a dental implant's surface. The implant was then exposed to a 940nm laser in continuous mode of varying wattages and times. This experiment confirmed that the bacteria could almost be eliminated from the implant surface by the use of a diode laser.

In a classic study performed by Ericsson et.al, [3] it was determined that at  $47\frac{1}{2}^{\circ}\text{C}$ , the bone would not integrate an implant properly or not at all. During a dental implant procedure, great care is taken to ensure that the bone temperature during drilling never exceeds  $47\frac{1}{2}^{\circ}\text{C}$ . This must extend to the treatment of peri-implantitis with a dental laser. If the treatment of a contaminated implant surface with a dental laser causes the surrounding bone temperature to rise above  $47\frac{1}{2}^{\circ}\text{C}$ , then that implant will likely be lost regardless of the treatment's decontamination success because the bone will lose its integration to the implant.

The most common reason for implant failure is periimplantitis. Periimplant disease refers to the pathological inflammation that occurs in the tissue surrounding an infected implant. These bacterial diseases are associated with symptoms such as increased pocket formation, bleeding, and mobility [4]. Titanium plasma sprayed implants increase implant-bone contact and anchorage force in the alveolar bone [5]. However, this also facilitates a surface to inhibit bacterial growth [6]. Many methods have been suggested to treat periimplantitis implants [7-10]. Mechanical debridement, antiseptics, antibiotics, surgical procedures, and explantation have been suggested therapy based

---

on the progress of the clinical case [11]. Plastic scalars have been proven as a safe method of debridement [12], while metal scalars and ultrasonic scalars have been shown to induce surface alteration in implants [13]. Bactericidal chemicals such as chlorhexidine gluconate as well as local and systemic antibiotics are useful adjuncts in the treatment of periimplantitis. The use of laser therapy has been discussed [14, 15] and now seems to be very promising [16-17]. Some lasers may not be suitable for the decontamination of implant surfaces because they cause considerable surface damage to the implant and the surrounding tissues [18]. In addition to surface damage caused by the radiation, heat is a major risk to the implant/bone integration. Temperatures in excess of 47-50°C cause significant damage to bone and tissue [19]. In several studies on the bactericidal effect of high-powered pulse laser radiation have shown to be a very effective method of debridement due to the fact that the laser energy is mostly absorbed by water. In bacteria, this causes cell lysis without damaging the surface of the implant. Many publications have shown the value of lethal photosensitization in decreasing the amount of viable pathogens without damaging the periimplant tissues [20, 21].

## Purpose

The purpose of this experiment is to determine if the technique of lethal photosensitization is practical for the treatment of a failing dental implant by measuring the change in temperature to observe if the temperature change as a result of radiation will cause the implant's surface to exceed the 47°C critical threshold.

## Hypothesis

It is predicted that over the 180 seconds of exposure, the 47°C critical temperature threshold will be exceeded after exposure to laser energy. This is so because significant charring was noted on implant surfaces after prolonged exposure to laser energy in previous studies.

## Procedures

1. A block of porcine femur of similar thickness to a human mandible is obtained.
2. Conventionally prepare and place a dental implant into a pig femur and create a bone defect to simulate the exposed implant surface of a diseased (peri-implantitis) implant.
3. Small holes in the bone adjacent to the dental implant are prepared, one immediately adjacent to the created osseous defect and another 180° opposite the defect. The thermocouple probe is inserted into each site to record the temperature changes.
4. The bone/implant is placed in a water bath maintained at 37°C to simulate the environment of the human body.
5. The exposed implant surface was exposed to the laser at wattages of 0.2, 0.5, 1.0, 1.5, and 2.0 in both continuous mode and in pulsed mode (20ms on- 20ms off) and the

temperature readings were recorded every 15 seconds for 180 seconds for each thermocouple site.

## Results

The data revealed that when exposed to radiation in continuous mode, the critical temperature of 47°C was exceeded at all wattages above 0.5. When the laser was set in pulsed mode (20ms on/20ms off), the temperature did not exceed the critical threshold with the exception of 2.0 watts. By using the pulsed interval setting, a higher wattage was able to be imparted to the implant surface and over a longer period of time without worry of exceeding the critical temperature. The temperature stopped increasing for pulsed intervals of exposure at approximately 165 seconds at both measured sites for 1.5 and 1.0 watts. In addition, the temperature measured at the 2 thermocouple sites about the implant demonstrated the same increases in temperature when exposed to the same laser energy.

## Conclusions

The hypothesis was rejected. Although some of the wattages did exceed the threshold, the use of lower wattages and the use of pulse interval exposure prevented temperatures from exceeding the critical threshold of 47°C. According to these results, the range of safe application of a 940nm GaAlAr laser to a dental implant surface is between 0.2-0.5 watts in continuous mode and 0.2-1.5 watts in pulsed (20ms/20ms) mode.

In addition, it can be concluded that the temperature elevation experienced by the implant and imparted to the adjacent bone will be uniform as both thermocouple sites recorded similar temperature changes under similar circumstances.

## Discussion

Using a pulsed interval versus a continuous interval on the same wattage would allow for maximum bacterial mortality while maintaining a low temperature. After comparing the data to the data of similar experiments performed with different laser systems, it is concluded that a pulsed setting will allow for optimum wattage output without exceeding the critical temperature. Although fairly accurate, the J/K-type thermocouple used has an error estimated at 1°C. The fiber-optic tip of the laser hand piece may have also had a newer or older tip, slightly changing the strength and accuracy of the beam. A porcine femur was used as it would have similar density, heat absorbing properties, and thickness to that of a human mandible. It also contained soft marrow on the inside just as a human jaw would. The laser was initiated before and after every trial. Future studies could examine the effect of a water mist or stream applied to the site as it is being lased in an effort to use a stronger wattage while minimizing temperature transferred to the implant and the surrounding bone. Although this new technique may improve the amount of bacteria killed in relation to the heating of the implant, the GaAlAs laser used in this study cannot allow any form of water to obstruct the beam or it will not function properly. In addition, other intervals of pulsed exposure may be varied which may allow for higher wattage to be used, again increasing the bactericidal effects of the laser. The burning look and odor as a

---

result of the lasing observed in previous studies may have been absent in this study due to the water bath which the implant was submerged or due to the fact that the heat could distribute itself through the bone and moderate the temperature of the implant, and thereby allow enough heat to be released that charring would not occur. This laser has not been tested for this purpose before. It did not harm the surface of the implant as other types of lasers have been shown to do and it also was able to impart a significant amount of energy without exceeding the  $47\frac{1}{2}^{\circ}\text{C}$  threshold. These results could lead to the introduction of this type of therapy into dental practices for the treatment of failing dental implants. This laser treatment could lead to more effective bacterial mortality with the least disturbance to the implant itself and its environment.

## References

1. "How Lasers Work." HowStuffWorks. 17 Sept. 2007 <http://science.howstuffworks.com/laser9.htm>.
2. Shibli, J A., M C. Martins, F S. Ribeiro, V G. Garcia, F H. Nociti, and E Marcantonio. "Lethal Photosensitization and Guided Bone Regeneration in Treatment of Peri-Implantitis: an Experimental Study in Dogs." *Clin Oral Implants Research* 3 (2007): 273-281. 3 Sept. 2007
3. Eriksson AR, Albrektson T. Temperature threshold levels for heat induced bone-tissue injury. A vital microscoping study in the rabbit. *J Prosth Dent* 1983;50:101-107
4. Mombelli A.: *Periodontol* 2000, 28, (2002) 177-189
5. Carlsson L, Rostlund T, Albrektsson B, Albrektsson T. Removal torques for polished and rough titanium implants. *Int J Oral Maxillofac Surg* 1998;3:21-42.
6. Fox SC, Moriarty JD, Kusy RP. The effects of scaling a titanium implant surface with metal and plastic instruments: An in vitro study. *J Periodontol* 1990;61:485-490.
7. Mombelli A, Land NP. *Periodontol* 2000, 17, (1998) 63-76
8. Mombelli A. "Proceeding of the 3rd Eutopean Workshop on Periodontology. Implant Dentistry ed. By N.P. Land, T. Karring, J. Lindhe (Quintessenz, Berlin, 1999) p.281-303
9. Baron M, Haas R, Dorbudak O, Watzek G. *Int J Oral Maxillofac Implants*, 15 (2000) 533-544
10. Klinge B, Gustafsson A, Berglundh T. *J Clin Periodontol*, 29, (2002) 213-225
11. Schou S, Berglundh T, Lang NP. *Int J Oral Maxillofac Implants*, 19, (2004) 140-149
12. Thomson-Neal DM, Evans GH, Meffert RM. Effects of various prophylactic treatments on titanium, sapphire and hydroxyapatite coated implants: An SEM study. *Int J Prosthodont Rest Dent* 1989;9:300-311
13. Ganz CH. Evaluation of the safety of the carbon dioxide laser used in conjunction with root form implants: A pilot study. *J Prosthet Dent* 1994;71:27-30
14. Masson ML. Using the laser for implant maintenance. *Dent Today* 1992;11:74-75
15. Haas R, Dorbudak O, Mensdorff-Pouilly N, Mailath G. Elimination of bacteria on different implant surfaces through photosensitization and soft laser. *Clin Oral Impl Res* 1997; 8:249-254
16. Kato T, Kusakari H, Hoshino E. Bactericidal efficacy of carbon dioxide laser against bacteria-contaminated implants and subsequent cellular adhesion to irradiated area. *Laser Surg Med* 1998;23:299-309
17. Block CM, Mayo JA, Evans GH. Effects of the ND:YAG laser on plasma sprayed and hydroxyapatite coated titanium dental implants *Int J Oral Maxillofac Implants* 1992;7:441-449
18. Romanos GE, Everts H, Nentwig GH. Effect of diode and ND:YAG laser irradiation on titanium discs. *J Periodontol* 2000;71:810-815
19. Kreisler M, Gotz H, Duschner H. Effect of the ND:YAG, Ho:YAG, Er:YAG, CO<sub>2</sub> an GaAlAr laser irradiation on endosseous dental implants. *Med Laser Appl* 2001;16:152
20. Shibli JA, Martins MC. *Journal of Oral Science*, 45 (1), (2003) 17-23
21. Coffelt DW, Cobb CM, MacNeill S, Rapley JW, Killoy WJ. *J Clin Periodontol*, 24, (1997) 1-7

---

# Where do Mouse Embryos Thrive Best? Comparison of Mammalian Embryo Development Under Varying Laboratory Environments

Yvonne K. Kao<sup>a</sup>, H. Lee Higdon III, Ph.D.<sup>b</sup>, Jennifer E. Graves-Herring, M.S.<sup>b</sup>, William R. Boone, Ph.D.<sup>b</sup>

<sup>a</sup>South Carolina Governor's School for the Arts & Humanities

<sup>b</sup>Department of Obstetrics and Gynecology, Greenville Hospital System University Medical Center, Greenville, SC

Received June 5, 2009

As the field of Assisted Reproductive Technology (ART) expands, so does the need to understand how differing laboratory environments affect development of embryos cultured *in vitro*. More specifically, do different air environments alter embryo development? To answer this question, we obtained mouse embryos from six hyperstimulated mice. The experiment was divided into two arms, with four replicates; half of the allotted embryos went to the ART clean room laboratory and the other half went to the non-clean room laboratory. The results of this experiment demonstrated that the clean room laboratory developed two-cell mice embryos to the blastocyst stage at a higher rate than those in the non-clean room laboratory. In conclusion, the results of this study indicate that improved air quality can promote better embryo development.

## Introduction

As the field of Assisted Reproductive Technology (ART) expands, so does the need to understand how differing laboratory environments affect development of embryos cultured *in vitro*. In theory, a sterile environment should provide the best possible chance for embryos to reach their full developmental potential. However, few prospective randomized trials addressing this issue exist in the scientific literature.

Two different laboratory environments, the ART clean room laboratory and the andrology laboratory, are used in the field of Assisted Reproductive Technology (Boone et al., 1999; Proctor et al., 2004). The ART clean room laboratory is a specially designed clean room that eliminates many particles in the air that may be harmful to human embryo development. The room is rated as a Class 100 clean room; therefore, no more than 100 particles of 0.5 microns or larger are in a cubic foot of air (Boone et al., 1999). In contrast, the andrology laboratory is not as efficient as the clean room because it is under HVAC control. Thus, the particle counts can reach in excess of 20,000 particles per cubic foot of air (Boone et al., 1999). These particles may carry unknown contaminants that may enter the culture media and affect embryo development.

The purpose of this study is to determine if air quality affects embryo development.

## Materials and Methods

*Clean Room Laboratory.* The clean room has four ultra low penetration air (ULPA) filters in the ceiling. Air is forced from the clean room through return vents located at the bottom of an exterior wall. The walls, ceiling, and floor of the clean room consist of nonshedding materials. Individuals that enter the clean room wear

Tyvek (Clean Wear Products, Toronto, Ontario) clothing to prevent shedding of particles.

*Andrology Laboratory.* The Andrology laboratory uses a standard airflow environment. The ceiling tiles are made of Celotex (Armstrong, Model Number 861; Armatuff, Greenville, SC). The walls are painted with a standard latex paint while the floor is a vinyl composite tile (Armstrong Imperial Excelon; Bonitzz, Greenville, SC). The ceiling tile, wall paint, and flooring material are not designed for clean room use and thus have a potential for shedding. Individuals enter the Andrology laboratory wearing street clothes.

*Incubator Environment.* Two incubators (Forma Scientific, Model Number 3158, Marietta, OH) were used for this study - one incubator in the clean room laboratory and one incubator in the andrology laboratory. Both incubators maintain the same, internal environment. The gas concentration for these incubators was 5% CO<sub>2</sub> and air, and the temperature was 36.7° C. Both incubators maintained a relative humidity in excess of 90%.

*Embryo Culture.* Two-cell embryos were obtained from six hyperstimulated mice (B6C3F1 strain). These two-cell embryos were cultured in 50 µL drops of Human Tubal Fluid (Irvine Scientific, Santa Ana, CA), covered with washed, equilibrated mineral oil (Humaco Mineral Oil; Aaron, Industries, Inc, Clinton, SC) residing in petri dishes (Model Number 3002, Becton Dickinson, Franklin Lakes, NJ). The embryos were grouped ten in each drop. After three days of culture, the embryos were checked for blastocoele development.

*Statistics.* This experiment was a prospective, randomized study. The experiment was divided into four replicates, performed on four separate days. One half of the allotted embryos were randomized to the clean room laboratory and the other half to the andrology laboratory. The blastocoele developmental rate was determined by the

number of blastocysts divided by the number of embryos allotted to each laboratory times 100%. Statistical tests were performed using Chi-square analysis.

## Results

As shown in Table 1, one hundred thirty-seven, two-cell mouse embryos were placed in each arm of the study. The blastocyst rate was significantly different ( $P=.01$ ) for these two study groups. Overall, two-cell mouse embryo development rates for clean room laboratory and andrology laboratory media were 99% (136/137) versus 93% (127/137), respectively.

## Discussion

In this prospective, randomized trial, we demonstrated that the environmental conditions in the clean room laboratory and the Andrology laboratory produced different results when we cultured two-cell mouse embryos to the blastocyst stage. The results of our study indicated that a clean room environment was more appropriate for culturing early mouse embryos than a standard laboratory.

Table 1: Comparison Between Mouse Embryo Development of

Replicate	Cleanroom	Andrology
	Laboratory	Laboratory
1	100% (39/39)	95% (37/39)
2	100% (20/20)	90% (18/20)
3	100% (30/30)	80% (24/30)
4	98% (47/48)	100% (48/48)
Total	99% (136/137)	93% (127/137)*

the Clean Room Laboratory and the Andrology Laboratory.

\* $P=0.01$ , Chi-Square Analysis

Cohen et al. (1997) performed studies on air quality in ART. As a result, they found common incidences of chemical air contamination caused by air pollutants. These air pollutants include volatile organic compounds (VOC), small inorganic molecules ( $N_2O$ ,  $SO_2$ , and  $CO$ ), substances derived from building materials, and other polluting compounds possibly released by pesticides

or aerosols. It has been determined that ART success rates decreased when embryo culture was performed in low air quality environments (Cohen et al., 1997).

Cohen et al. (1997) have indicated that allowing the emission of gases from new laboratory equipment was crucial. They demonstrated that air extracted from new incubators reveal concentrations of VOC that were 100 fold greater than air extracted from incubators that had been in use. They suggested that outside air may be a cleaner source of air than inside, for outside air is relatively VOC free. They further suggested that fixed and transient laboratory components may produce gaseous emissions. In addition, they cautioned against the use of detergents and alcohol-based scrubs in cleaning laboratory equipment since their efficacy is dubious, especially if they are implemented in order to substitute for poor sterile technique.

In the future, several other studies ought to be conducted. One such study should be a multi-center trial to validate these findings. A second study should investigate development past the blastocyst stage. In order to do this, blastocysts from both arms of the study should be transferred to recipient mice and allowed to develop to term and observations made upon the live offspring to determine if there are significant differences.

In conclusion, our study demonstrated that air quality plays a significant role in the development of mammalian embryos. Thus, we would recommend that individuals that culture mammalian embryos consider monitoring air quality and improving it when necessary.

## References

1. Boone WR, Johnson JE, Locke AJ, Crane MM, Price TM. Control of air quality in an assisted reproductive technology laboratory. *Fertil Steril* 1999;71:150-4.
2. Cohen J, Gilligan A, William E, Schimmel T, Dale B. Ambient air and its potential effects on conception *in vitro*. *Human Reproduction*. 1997;12:1742-9.
3. Proctor JG, Blackhurst DW, Boone WR. Does seasonality alter intrauterine insemination outcomes: a 5-year study. *J Assist Reprod Gen*. 2004;21:263-9.

---

# The effect of omega-3 fatty acid (n-3) concentrations on the sustainability of astrocytoma cells when exposed to 1-methyl-4-phenyl-1,2,3,6-tetrahydropyridine

Nancy Zhong

Spring Valley High School, 120 Sparkleberry Lane, Columbia, SC 29223

Received August 25, 2009

Astrocytes are a type of glial cell located in the brain apart of the nervous system. Their major job is directly function with neurons: modulate the environment around neurons, release a range of neuronal growth factors, and help maintain the cellular barrier between blood and brain. (Svendsen, 2002). When a neuron is damaged by a toxin, such as in Parkinson's disease, the astrocyte population grows rapidly around the other neurons in order to protect them. They take up the toxin and transform it into a byproduct (MPTP to MPP+). However, the new byproduct produced is shown to play a role in the sequence of events leading to a dopamine neuronal cell and astrocyte death (Wong et al., 1999). Champeil-Potokar et al. conducted a study on the effect of astrocyte cultures in DHA, a n-3 polyunsaturated fatty acid which showed that astrocytes cultured in medium plus DHA had a more physiological n-3 status, grew better, and retained their astrocyte phenotype, with changes to the phospholipids membrane. Therefore astrocytes are physiologically relevant provided with adequate DHA. In this research, omega-3 fatty acid was tested to see its effects on the astrocytoma, cancer form of astrocytes, from the toxin, MPTP, through possible manipulation in the plasma membrane. It was hypothesized that as more omega-3 fatty acid was added to the cells there would be stronger resistance to the toxin. A one-way ANOVA was used to test the significance. It was found that the p-value was less than 0.001 and then the Tukey's test showed that there was a significant difference between all of the tested variables. However it was a decreasing correlation, which did not support the hypothesis, but it is still very significant to the relationship between astrocytes and DHA.

## Introduction

Currently in America, 1.5 million people are diagnosed with Parkinson's and there are 60,000 new cases joining that number annually. It is a brain disorder, occurring in certain neurons, in the part of the brain called the substantia nigra, which die or become injured (NPF, 1997). In Parkinson's disease, the neurons begin to deteriorate (at least 80%) and this causes a lot of problems in coordinated functioning of body's muscles and movements. (NPF, 1997). There is no cure for the Parkinson's disease. However there are products available to help ease the tremors.

Astrocytes are type of glial cell located in the brain apart of the nervous system. They major goal is functioning with neurons. Astrocytes modulate the environment around neurons, release a range of neuronal growth factors, and help maintain the cellular barrier between blood and brain. Recent studies also show that they help in the regeneration of neurons known as neurogenesis (Svendsen, 2002). When a neuron is damaged by a toxin such as in Parkinson's, the astrocyte population grows rapidly around the other neurons in order to protect them from further damage. They also take up the toxin and transform it into another byproduct (MPTP → MPP+). However, the new byproduct produced is shown to play a role in the sequence of events leading death to a dopamine neuronal cell. (Wong et al., 1999)

Long-chains of polyunsaturated fatty acids, mainly docosahexaenoic acid (DHA) and arachidonic acid, are fundamental constituents of cell membrane phospholipids. DHA is found to be vital for cognitive function, especially when people age. It has impact on behavior and learning and is critical for proper neural development in infants. However little is known about the role of DHA in astrocyte functioning (Jensen, 2002).

In the Rotterdam study, dietary fatty acids were tested against Parkinson's incidence through statistical analysis. PD was evaluated among 5289 people and monounsaturated fatty acids (MUFAs) and polyunsaturated fatty acids (PUFAs) intakes were significantly associated with a lower risk of PD. The results concluded that unsaturated fatty acids are important to neurons because of its neuroprotective, anti-inflammatory, and antioxidant properties (de Lau et al., 2005). In the 2007, a study was done at Laval University on mice, copying the effects of omega-3 polyunsaturated fatty acids on an induced neuron-degenerating disease. The researchers observed that when the mice were fed an omega-3 rich diet, they appeared immune to MPTP. So omega-3 fatty acid will be used in the experiment, because of it has potential to be resistant to toxins. MPTP is a toxin that affects in the same way as Parkinson's disease (Bousquet et al., 2008) so it will also be used in experimentation.

Champeil-Potokar et al. did a study on the effect of astrocyte cultures in DHA, an n-3 polyunsaturated fatty acid. It showed that astrocytes cultured in medium plus DHA had a more physiological n-3 status, grew better, and retained their astrocyte phenotype. Therefore astrocytes are physiologically relevant provided with adequate DHA. At certain amounts there was no effect but with large amounts were incorporated there showed to greatly altered the phospholipids of the membrane. The amounts that they used in this experiment were 60uM and 30uM DHA.

So omega-3 fatty acid will be used to see if there is a possibility that it will help to protect the astrocytes in the presence of MPTP, by altering the membrane making them capable to clean up the toxins. It is hypothesized that there will be more astrocytes with the omega-3 fatty acid (DHA) present than without it. The MPTP alone should make kill all of the astrocytes, so there are none in that dish. The experiment is done through the

use of hemocytometer and microscope, to physically count the individual cells. Also, because of financial reasons, astrocytes were not used but instead the more rapid growing cancer version, astrocytoma cells were used.

## Methods

First the astrocytes were taken and put into a water bath to be unfrosted at 37C. Then they were put into petri dishes with 10mL of medium and 1mL of 10% FBS serum and let were grown in incubator. After four days the dishes were taken out and 1mL of trypsin was added—this was done to detach the cells from the plate—for 3 minutes. Then with 10% DMEM, the cells were suctioned in and out of the micropipette 10 times. They were then pipetted from the dish into a purple-caped tube. The tube was shaken; then a 1uL sample was taken from the tube and pipetted in a hemocytometer. The hemocytometer was placed under the microscope and the initial readings were taken. This process was done 3 times. A diagram of the hemocytometer is shown in Figure 1. The cells were then counted from left to right, up to down, shown by the arrows.

The averages of the four boxes for the 3 trials were taken for the initial trials before anything else was done to the cells. Four plates were taken and then 15mL of the cells were taken from the purple tube and put onto each plate. In the first plate nothing was added. In the second (toxin only), third, and

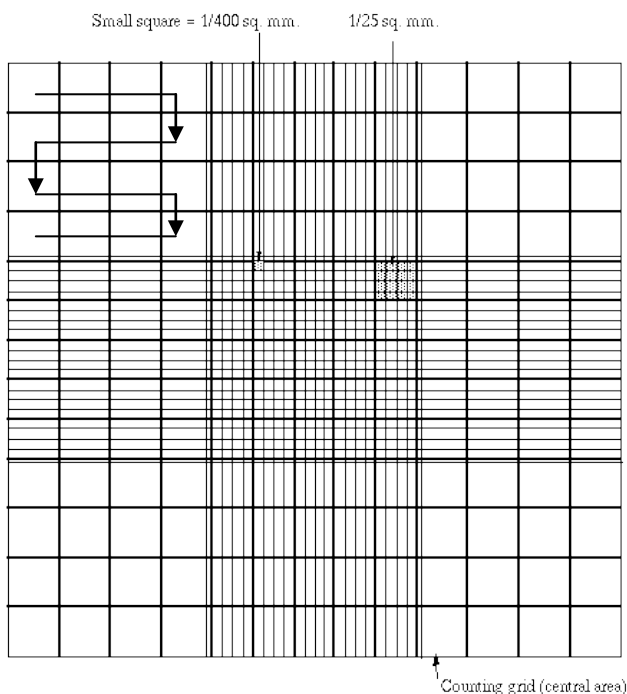


Figure 1: Zoomed image of hemocytometer under a microscope. The arrows show the direction in which you would count the cells. The hemocytometer are split into four boxes, shown by the darkened lines. The cells would be counted for each of the boxes and averaged to created a total number of cells per .1uL

fourth plates, 6.4uL of MPTP were added. Then in the third plate,

Source	DF	SS	MS	F	P
Factor	3	16719.6	5573.2	126.19	< 0.001
Error	8	353.3	44.2		
Total	11	17072.9			

30M of DHA was added to the cells. And finally in the fourth plate, 60M of DHA was added. The plates all received nutrients and were set in for incubation for 1 week.

After the week the cells were taken and put through the

IV: amount of omega-3 fatty acid—DHA (g)	Control (no MPTP, no DHA)	0uM DHA (Toxin only)	30uM DHA	60uM DHA
Number of trials:	3	3	3	3

same process of counting and the results were jotted down in Table 1. Then a one-way ANOVA was done on the results to test the significance.

Table 1. Experimental design diagram. DV: number of cells counted. Constant: amount of MPTP (excluding the control), begin with the same starting amount of astrocytes (6 cells), same size Petri dish, same amount of nutrient

The averages of the four boxes for the 3 trials were taken for the initial trials before anything else was done to the cells. Four plates were taken and then 15mL of the cells were taken from the purple tube and put onto each plate. In the first plate nothing was added. In the second (toxin only), third, and fourth plates, 6.4uL of MPTP were added. Then in the third plate, 30M of DHA was added to the cells. And finally in the fourth plate, 60M of DHA was added. The plates all received nutrients and were set in for incubation for 1 week.

After the week the cells were taken and put through the same process of counting and the results were jotted down in Table 1. Then a one-way ANOVA was done on the results to test the significance.

## Results

After the cells were counted the numbers were recorded in the table below (Table 1). Three dishes in each interval were collected to reduce bias.

# of cells/.1uL					
Trials	Initial	Control	Toxin only	30 uM DHA	60 uM DHA
Trial 1	90	117	67	61	14
Trial 2	64	113	92	54	10
Trial 3	68	115	80	58	12

Table 2: The number of cells counted in each of the test groups; there is a general downward trend when concentrations of DHA increase.

Confidence intervals were calculated at a 95% confidence for each interval and the pooled standard deviation was calculated (see appendix). Then a one-way Analysis of Variance (ANOVA) test (unstacked) was conducted to test the significance of the results (Table 2). Because the F-value was so much bigger than the table value p-value at 95% confidence is less than 0.000 the statistics of the results are significantly different and it is reasonable to conclude that there was a pattern. Now a graph was plotted to show the how the pattern was correlated.

Because there was significance in the results, a Tukey test was conducted to determine where the significant differences lay. There was no zero in the confidence intervals between the groups meaning that the results were all found to be significant (for Tukey's test details, see appendix).

Table 3: results of one-way ANOVA; the p-value shows there is significance in the results; Tukey must be done now to show where the results are.

The means of each interval were taken and plotted on a graph shown in Figure 2. It was shown that the graph has a negative slope.

## Discussion

The one-way ANOVA and the Tukey test found the results to be significant, meaning there was a significant difference between the trials. However the significance lies in an inverse relationship between the amount of DHA and number of cells counted, because of the graph represented in Figure 2.

The original hypothesis was that there would be an increase in the number of astrocytes because the fatty acids would create a stronger resistance to the toxin. However the results, shown in Table 1, and the graph, in Figure 2, did not support this hypothesis. Instead the results show a significant *decrease* when concentrations of omega-3 fatty acid were added to the samples.

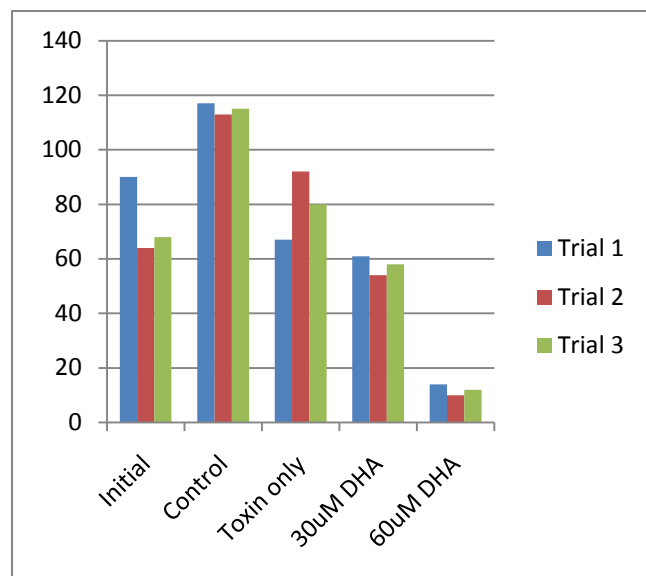


Figure 2: Graph of the counted cells under the hemocytometer; As shown the control grew, the toxin stayed the around the same, 30uM and 60uM both decreased

This experiment contradicted many of the previous studies. However the studies done in the past were *in vivo*; this was an *in vitro* study. Many of the previous experiments showed that astrocytes grew better in medium plus DHA (Champeil-Potokar et al., 2004). But in these experiments, results stated that the two main classes of membrane phospholipids were greatly altered (Champeil-Potokar et al., 2004). And Bousquet et al. said that if there wasn't enough PUFA (polysaturated fatty acids) than there would be no effect and that at high levels the n-3 PUFA diet protected against MPTP-induced decrease in dopamine. However in this experiment even at 60M of DHA there was a *negative* effect. It can be inferred that the n-3 fatty acids were taken up by the astrocytes and incorporated into the membrane of the cells. This may have a negative effect to the cell's general function.

In other research it was found that the MPTP that was accumulated in astrocytes was converted to its toxic metabolite,

1-methyl-4-phenylpyridinium ion (MPP+) by the enzyme monoamine oxidase B (MAO-B), which is predominate in astrocytes (Wong, et al., 1999). The astrocytes showed to have a high capacity for MPP+ retention and efflux. That made them more resistant to the MPTP. But when the DHA was incorporated into the membranes of the astrocytes, this made them less prone to take up the MPTP and therefore they could not make the MPP+ as a byproduct. Like peroxisomes in animal cells, the astrocytes are the digesters of toxin in the brain. However if they were to become incapable of picking up the toxin then they would also be more vulnerable to the negative effects of the toxin. This explains why there was a decrease when the DHA concentrations were added to the astrocytes.

This may be a link that DHA is not as good at protecting the astrocytes, because it hinders their capability to catalyze the MPTP. However there was no test on how DHA affects the neural cells, so nothing can be said about how DHA will affect the whole individual. But it can be stated that as the levels of DHA increased, the survival rate of astrocytoma cells went down significantly.

In this experiment, instead of astrocytes, astrocytoma cells were used. This may also have affected the outcome of the experiment. For the experiment, astrocytoma cells were used because they would grow at a faster pace and so the experiment would have a larger sample size than using the normal astrocytes. However because the cells were not exactly the same, they could have reacted differently to the treatments that were given. It may be that the DHA inhibited the growth of the astrocytoma cells because their membranes were modified differently than the astrocytes because they were made to produce faster.

There was also an increase in the toxin only trial, which was not initially expected. But looking into more experiments it makes more sense as to why there would be such a growth of astrocytes when the MPTP was added. Astrocytes have a very close relationship to neural cells. It was also shown that astrocytes can instruct unspecialized cells to become neurons—a process called neurogenesis (Svendsen, 2002). Astrocytes are there to protect the neurons; if in the presence of MPTP a neuron were to be damaged, the population of astrocytes would go up—in order to protect the other neurons which have not yet been damaged (Wong et al., 1999).

In this experiment, very rudimentary in the techniques, so there is a possibility that the physical task of counting may have led to error: human error. However it seems very possible that the astrocytes would be more susceptible to dying in the presence of the DHA because it would not be allowed to recognize the MPTP since the plasma membrane's conformation was altered.

In the future, it would be more interesting to test neurons and DHA directly. There would be a different association in the presence of MPTP, according to previous research. Or possibly test astrocytes against different types of omega-3 fatty acids, i.e. n-6. There might be different outcomes in their mortality.

## Acknowledgements

I would like to thank Xin Yang Yang for helping me get in touch with the equipment at Cokes Center at University of South

---

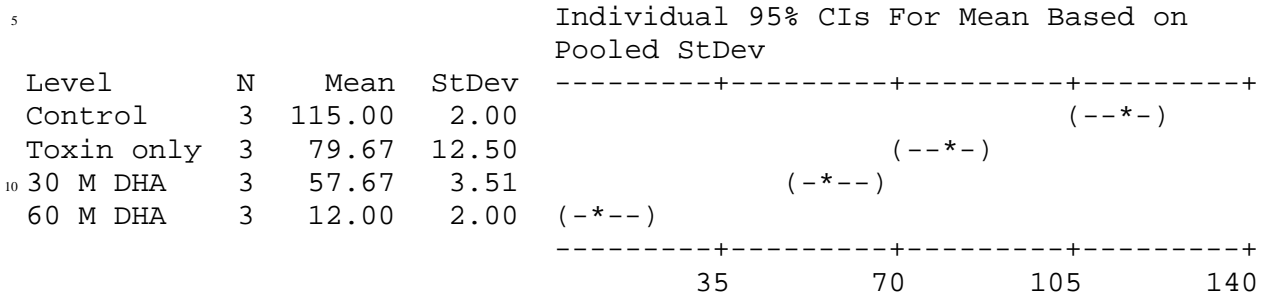
Carolina. I would also like to thank my dad for encouragement and mom for support. Thanks to Mrs. Spigner for helping me with my paper and presentation. Thanks to Mrs. Castillo and Mr. Soblo for helping me with statistical analysis. And thanks to the South Carolina Junior Academy of Science for financial help.

## References

1. About Parkinson disease. National Parkinson Foundation. (1997) 21 October 2008. <http://www.parkinson.org/NETCOMMUNITY/Page.aspx?pid=225&srcid=201>.
2. Bousquet M., Saint-Pierre, M., Julien C., Salem, N., Cicchetti F., Calon F. (2008) Beneficial effects of dietary omega-3 polyunsaturated fatty acid on toxin-induced neuronal degeneration in animal model of Parkinson's disease. *The FASEB Journal* 22, 1213-1225.
3. Champeil-Potokar, G., Denis, I., Goustard-Langelier, B., Alessandri, J.M., Guesnet, P., Lavialle, M. (2004) Astrocytes in culture require docosahexaenoic acid to restore the n-3/n-6 polyunsaturated fatty acid balance in their membrane phospholipids. *Journal of Neuroscience Research* 75, 96-106.
4. De Lau, L.M.L., Bornebroek, M., Witteman, J.C.M., Hofman, A., Koudstaal, P.J., Breteler, M. (2005) Dietary fatty acids and the risk of Parkinson disease. *Neurology* 64, 2040-2045.
5. Jensen, A.W. (2002) DHA is essential for brain function, heart, health, and more. Retrieved January 2, 2009, from Life Enhancement: [http://www.life-enhancement.com/article\\_template.asp?id=686](http://www.life-enhancement.com/article_template.asp?id=686)
6. Kato H., Kurosaki R., Oki C., and Araki T. (2004) Arundic acid, an astrocyte-modulating agent, protects dopaminergic neurons against MPTP neurotoxicity in mice. *Brain Research* 1030, 66-73.
7. Moore, S. (2000) Polyunsaturated fatty acid synthesis and release by brain-derived cells in vitro. *Journal of Molecular Neuroscience* 16, 195-200.
8. Svendsen C. N. (2002) Neurobiology: the amazing astrocyte. *Nature* 417, 29-32.
9. Wong S.S., Li R.H.Y., and Stadlin A. (1999) Oxidative stress induced by MPTP and MPP<sup>+</sup>: selective vulnerability of cultured mouse astrocytes. *Brain Research* 836, 237-244.

APPENDIX

S = 6.646 R-Sq = 97.93% R-Sq(adj) = 97.15%

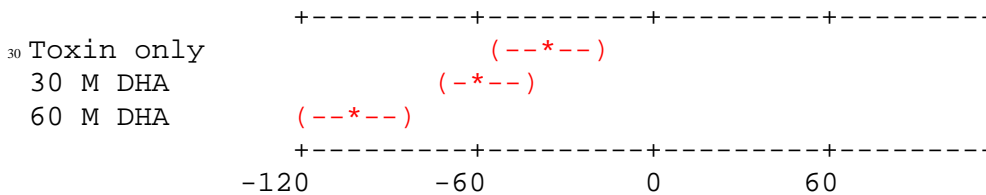


15 Pooled StDev = 6.65

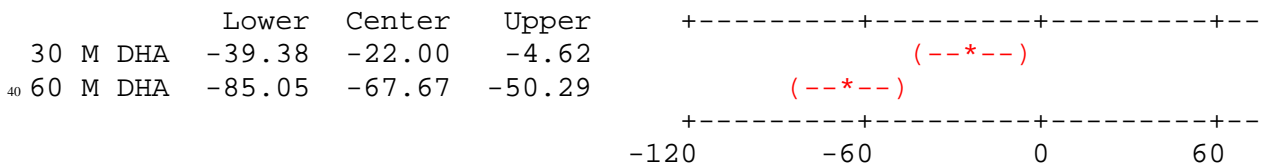
Tukey 95% Simultaneous Confidence Intervals  
All Pairwise Comparisons

20 Individual confidence level = 98.74%  
(the red marks the relationships that are significantly different)  
Control subtracted from:

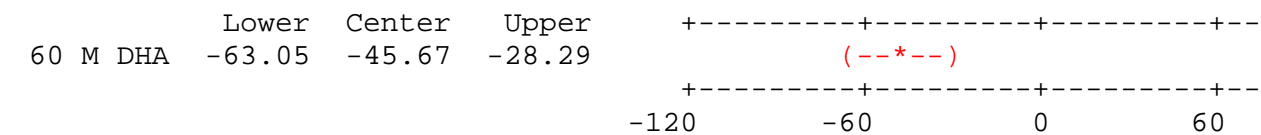
	Lower	Center	Upper
25 Toxin only	-52.71	-35.33	-17.95
30 M DHA	-74.71	-57.33	-39.95
60 M DHA	-120.38	-103.00	-85.62



35 Toxin only subtracted from:



30 M DHA subtracted from:



50